Graphene Nanoplatelets-Based Advanced Materials and Recent Progress in Sustainable Applications

DOI:
10.3390/app8091438

Document Version
Final published version

applied sciences

MDPI

Review

Graphene Nanoplatelets-Based Advanced Materials and Recent Progress in Sustainable Applications

Pietro Cataldi *, Athanassia Athanassiou and Ilker S. Bayer

Smart Materials, Istituto Italiano di Tecnologia, Via Morego 30, 16163 Genova, Italy; athanassia.athanassiou@iit.it (A.A.); ilker.bayer@iit.it (I.S.B.)

* Correspondence: pietro.cataldi@iit.it

Received: 5 July 2018; Accepted: 15 August 2018; Published: 23 August 2018

Abstract: Graphene is the first 2D crystal ever isolated by mankind. It consists of a single graphite layer, and its exceptional properties are revolutionizing material science. However, there is still a lack of convenient mass-production methods to obtain defect-free monolayer graphene. In contrast, graphene nanoplatelets, hybrids between graphene and graphite, are already industrially available. Such nanomaterials are attractive, considering their planar structure, light weight, high aspect ratio, electrical conductivity, low cost, and mechanical toughness. These diverse features enable applications ranging from energy harvesting and electronic skin to reinforced plastic materials. This review presents progress in composite materials with graphene nanoplatelets applied, among others, in the field of flexible electronics and motion and structural sensing. Particular emphasis is given to applications such as antennas, flexible electrodes for energy devices, and strain sensors. A separate discussion is included on advanced biodegradable materials reinforced with graphene nanoplatelets. A discussion of the necessary steps for the further spread of graphene nanoplatelets is provided for each revised field.

Keywords: graphene nanoplatelets; flexible electronics; wearable electronics; strain sensor; structural health monitoring; stretchable electronics; reinforced bioplastics

1. Graphene and Graphene Nanoplatelets

Graphene is a single freestanding monolayer of graphite [1]. It is the first 2D-material ever manufactured by mankind, having a thickness of one atom (0.34 nm), and lateral size orders of magnitudes larger [2–4]. Graphene combines diverse and unique physical properties (see Figure 1), and as a result, is an ideal building block for miniaturized next-generation devices, with applications in fields like photonics, opto-electronics, protection coatings, gas barrier films, and advanced nanocomposites [5–7].

In recent years, many studies have focused on solutions to conveniently mass-produce defect-free graphene. More than twelve different fabrication techniques were proposed [6,8–13]. Two noteworthy processes are chemical vapor deposition on copper or metals [14] and liquid phase exfoliation of graphite [15]. The first method is a bottom-up approach: it makes wide graphene films grow on top of metallic foils, starting from volatile carbon based precursors. In contrast, liquid phase exfoliation is a top-down method which singles out the graphene monolayer by sonicating graphite immersed into solvents with low surface tension or water with surfactants [15,16]. Single layer graphene flakes are then isolated only after additional ultracentrifugation steps.

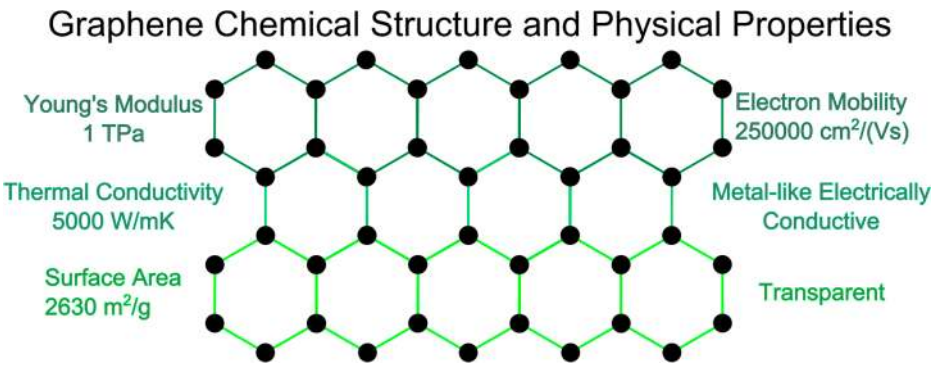

Figure 1. Graphene hexagonal honeycomb chemical structure and its remarkable physical properties. The black dots are carbon atoms.

Pure graphene is not yet mass-produced though. There is still a lack of a large scale manufacturing techniques that isolate these 2D crystals with the same outstanding performance as that required to produce the samples fabricated in research laboratories [10]. The main limitations are the low fabrication rates and high sales costs. On the other hand, graphene nanoplatelets (also known as graphite nanoplatelets, GnPs, or GPs) combine large-scale production and low costs with remarkable physical properties. This nanoflakes powder is normally obtained following the liquid phase exfoliation procedure without further centrifugation steps. Other widespread GnP manufacture methods are ball-milling [17], the exposure of acid-intercalated graphite to microwave radiation [17], shear-exfoliation, and the more recent wet-jet milling [18]. These manufacturing techniques produce a large variety of powders in terms of thickness, lateral size of the flakes, aspect ratio, and defect concentrations [18]. GnPs are composed of single and few layer graphene mixed with thicker graphite (see Figure 2); hence, structurally they are in between graphene and graphite. In literature, graphene based materials are classified according to their thickness, lateral size, and carbon to oxygen atomic ratio [19]. Considering the morphological characteristics, the graphene family can be classified as single layer graphene, few layer graphene (2–10 layers), and graphite nano- and micro-platelets. Commercially available GnPs are a mixture of single layer, few layers, and nanostructured graphite. In other words, GnPs thickness can vary from 0.34 to 100 nm within the same production batch [20,21]. Note that graphite is typically considered a 2D-like material (i.e., not bulky) when its number of layers is $\leq$10 [10].

GnPs exhibit exciting properties such as light weight, high aspect ratio, electrical and thermal conductivity, mechanical toughness, low cost, and planar structure. As such, they are attractive options to replace different nanostructured fillers in material science, such as other carbon allotropes (i.e., carbon black or carbon nanotubes), metallic nanoparticles, and clay [21,22]. They are appealing for nanocomposites, since they can easily and successfully be included in polymeric matrices by solvent or melt compounding [23]. GnPs are cheaper than carbon nanofibers and nanotubes, and are comparable with such tube-like nanofillers in modifying the mechanical properties of polymers [21,24]. Moreover, GnPs' electrical conductivity is orders of magnitude higher than those of graphene oxides [25].

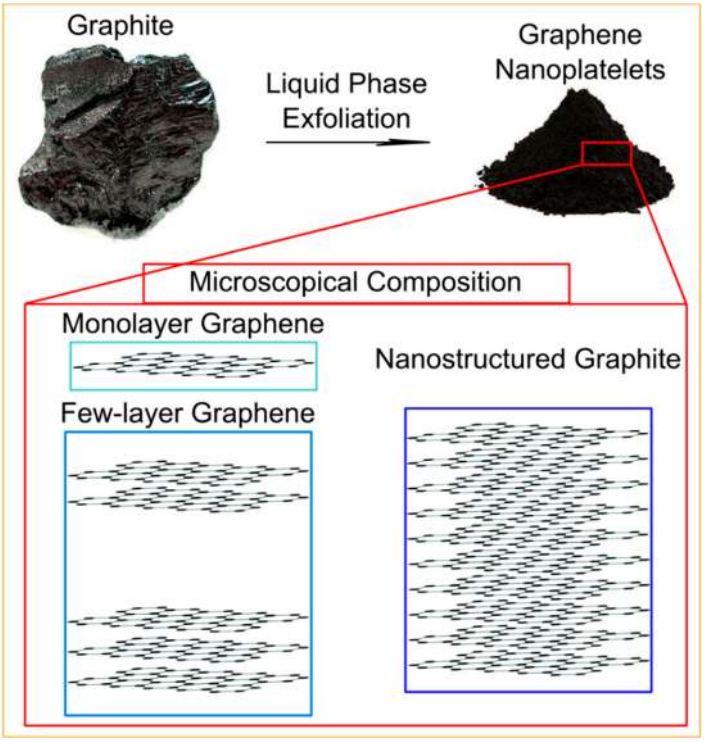

Figure 2. Schematic of the manufacture of GnPs starting from natural graphite. The typical black powder obtained after liquid phase exfoliation and solvent evaporation is constituted by a mixture of single and few layer graphene and nanostructured graphite.

Considering this, graphene nanoplatelets are already employed in several technological fields. In fact, GnPs-based materials show increased tribology [26,27], mechanical [17,28–31], biomedical [32–34], gas barrier [35,36], flame retardant [37,38], and heat conduction [39–42] properties. Furthermore, GnPs can transform plastic in an electrical conductor, converting it into a conformable material for electronics [43–45]. Finally, GnPs showed good potential for enhancing the thermal conductivity of polymer matrixes [46], making them suitable as thermal interface materials [39,47].

In this review, we will focus on GnP-based applications related in areas such as flexible and wearable electronics, motion and structural sensors, and reinforced bio-nanocomposites. In particular, we will show that GnPs unveils large-scale and unique uses (from antennas to energy harvesting) in the field of flexible electronics. We will discuss the potential uses of GnPs in smart fabrics, and the steps needed to reach a wide distribution of wearable technology. We will display many different approaches and materials employed to fabricate strain and pressure sensors, structure health monitoring systems, and stretchable devices. Finally, we will present recent advances in the field of GnP-reinforced bioplastics, and the potential of these nanoflakes to fill the performance gap between long-lasting traditional plastics and green and sustainable biopolymers.

2. Flexible Electronics Based on GnPs

Most electronic devices are based on rigid inorganic components. These conventional materials present drawbacks in light of the rise of applications that require flexibility, such as artificial electronic skin, wearable and compliant electronics, and portable energy harvesting devices [48]. The combination of the mechanical properties of polymers and conductive nanofillers is promising as a way of creating flexible and compliant conductive materials. In particular, investigation into polymers combined with silver nanoflakes showed encouraging results in flexible electronics [49]. However, nano-silver's high cost limits its large-scale production [50].

In such a context, carbon-based conductive nanofillers, and in particular, graphene nanoplatelets, gained increased attention as materials for flexible electronics due to their flexibility and low sheet resistance, i.e., that can reach the order of Ω/sq [43]. Different approaches were developed (see Table 1).

Table 1. Flexible Electronics GnPs-based. We report the manufacturing technique, electrical conductivity (EC) or sheet resistance (SR), durability tests performed and references. EC and SR are related by this formula: EC = 1/(SR × t) where t is the thickness of the material. PMMA stays for poly(methyl methacrylate), PET for polyethylene terephthalate, PTFE for polytetrafluoroethylene, PDMA for polydimethylsiloxane and PEDOT:PSS for poly(3,4-ethylenedioxythiophene) polystyrene sulfonate.

Type of Sample	Manufacturing Techniques	EC (S/m) SR (Ω/sq)	Durability Tests	Reference
Freestanding GnPs	Water dispersion and filtration	2×10^6 S/m	Not reported	[36]
GnPs-Polycarbonate Composite	Extrusion	2×10^{-6} S/m	Not reported	[51]
GnPs-Nylon 6,6 composite	Solution blending	1 S/m	Not reported	[52]
GnPs coupled with ionic liquid ions and epoxy	Solution blending and curing	10^{-3} S/m	Not reported	[53]
Polyimide substrate functionalized with GnPs	Drop casting	Not reported	Not reported	[54]
Glass, Al_2O_3 and PET substrates functionalized with PMMA-GnPs paste	Screen printing	20 kΩ/sq	Not reported	[55]
Transparent substrates coated with GnPs-PEDOT:PSS	Ink-jet printing	2×10^2 S/m	Bending (ammonia sensor)	[56]
GnPs-functionalized paper	Screen printing and rolling compression	4×10^4 S/m	Bending (antenna)	[57]
GnPs-acrylic paint emulsion on paper	Spray coating, heat-curing and polishing	5×10^2 S/m	100 abrasion and peeling	[58]
GnPs-functionalized paper	Filtration via PTFE membrane and transfer printing process	Not reported	1000 folding cycles at 180° and −180° bending angle	[59]
Deposition of GnPs on polymeric substrates, cardboard or textiles	GnPs compression with hydraulic press and lamination on different substrates	10^5 S/m	Hundreds of thousands bending cycles at bending radii of 45 and 90 mm	[60]
GnPs on PMMA with silver nanowires	GnPs brush coated on PMMA and silver nanowires sprayed on top. All the structure embedded on PET or PDMS	12 Ω/sq	100,000 bending cycles with minimum bending radius of 5 mm and stretching up to 50%	[61]
Cellulose impregnated with GnPs/Mater-bi conductive ink	Spray and Hot-pressing	10^3 S/m 10 Ω/sq	Tens of 180° folding-unfolding cycles at 0 mm bending radius.	[43]
Cellulose impregnated with GnPs/Mater-bi conductive ink	Spray and Hot-pressing.Lamination on top of a solar cell	10 Ω/sq	Solar Cell performance after bending-unbending	[62]
Cellulose impregnated with cellulose acetate and GnPs	Spray and self-impregnation	10^3 S/m 10 Ω/sq	Abrasion cycles (30 min) and tens of 180° folding-unfolding cycles at 0 mm bending radius	[63]
GnPs and nanofibrill cellulose into PLA and Polypyrrole	Solution processing	106 S/m	100 bending cycles at 180° bending angle	[64]

One method consists of fabricating freestanding GnP-based materials. Wu et al. [36] fabricated a flexible and light-weight self-standing graphene nanoplatelets paper, reaching the remarkable electrical conductivity of $\sigma \approx 2 \times 10^6$ S/m. This binder-free porous film was bent without ruptures, as shown in Figure 3. It was impregnated with both thermoset and thermoplastic polymers to increase its mechanical properties. After this impregnation procedure, the GnP paper displayed a reduced electrical conductivity ($\sigma \approx 7 \times 10^5$ S/m). Coupling with carbon fibers diminished its sheet

resistance and enhanced its thermal properties. The GnPs employed by Wu et al. were prepared in their laboratory.

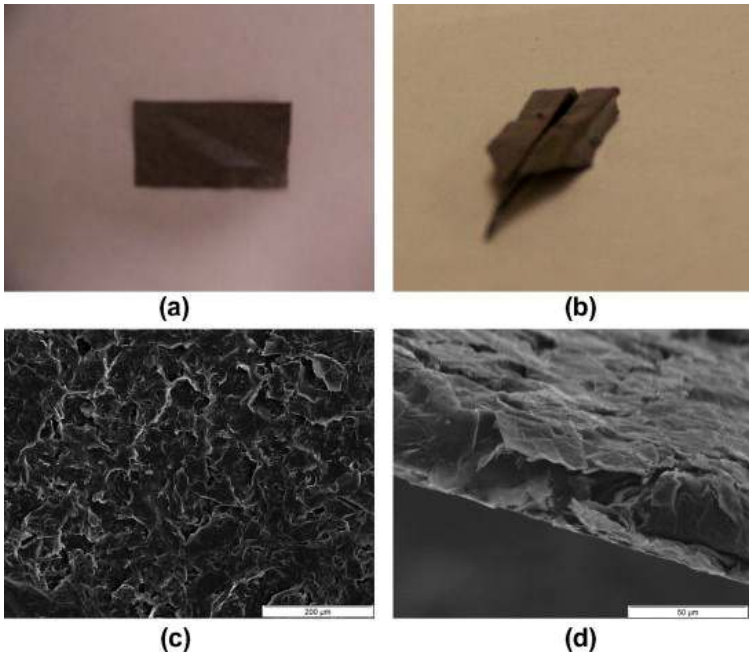

Figure 3. Self-standing GnPs paper and its flexibility. (**a**,**b**) are photographs of the paper before and after folding. (**c**,**d**) are SEM images of the morphology of the surface of the GnPs paper (plane and at the folding edge, respectively). Reprinted with permission from Carbon 50, 3, 1135–1145. Copyright 2012 Elsevier.

Although promising, the manufacture of freestanding GnPs substrates is often complicated and difficult to scale-up. Therefore, scientists explored other approaches depending on the type of polymer employed (i.e., thermoplastic or thermoset). For example, the incorporation of GnPs in thermoplastic polymer matrices led to flexible and conductive materials. Following this procedure, King and collaborators [51] extruded polycarbonate-GnPs nanocomposites with improved electrical properties. Such materials preserved ductile and plastic behavior up to 8 wt % GnPs concentration, and exhibited an electrical conductivity of approximately 2.5×10^{-6} S/m. Papadopoulou et al. [52] designed a new solvent mixture (trifluoroacetic acid and acetone) for flexible thermoplastic nylon 6.6 graphene nanoplatelets nanocomposites. They used a solvent casting method to fabricate the films. At 20 wt % nanofiller concentration, the material showed an electrical conductivity six orders of magnitude higher than that obtained by King and collaborators ($\sigma \approx 1$ S/m). They also demonstrated that, by incorporating GnPs, the pure nylon matrix improved the Young's modulus more than twice. Papadopoulou et al. employed commercially available GnPs obtained from Directa Plus (Lomazzo, Italy) (grade Ultra g+). Such GnPs were characterized in depth in our previous work [65]. Recently, Hameed and coauthors [53] proved that the use of ionic liquid induces flexibility in brittle thermoset matrices, and improves the dispersion of GnPs. Such modified thermoset polymers displayed enhanced tensile strength and Young's modulus, and were electrically conductive ($\sigma \approx 10^{-3}$ S/m).

2.1. GnPs Functionalized Substrate

Another promising approach for flexible electronics is the functionalization of bendable substrates with GnPs-based conductive ink. Tian et al. [54] fabricated temperature-dependent resistors by simple drop-casting of conductive GnPs suspensions on polyimide. Such temperature sensors were stable at high relative humidity conditions, and performed more efficiently compared to carbon nanotubes

devices. Printing and spraying of conducting inks are convenient techniques to functionalize substrates, since the necessary tools are already largely diffused in the manufacturing industry [50,66]. Indeed, researchers took advantage of both methods to functionalize different flexible materials employing GnPs as conductive nanomaterials. For example, Wróblewski and Janczak [55] screen-printed flexible paste made of PMMA-GnPs, realizing electrodes on diverse substrates (glass, Al_2O_3, PET). This conductive paste, made with 1.5 wt % GnPs, had a sheet resistance in the order of 20 kΩ/sq, and transparency near 17%, enough to utilize this coating as an electrode for electroluminescent displays. Seekaew and coauthors [56] ink-jet printed conductive GnPs-PEDOT:PSS dispersion on top of a transparent substrate, manufacturing a sensor for ammonia detection. The fabrication steps and the obtained device are presented in Figure 4. The addition of only 2.33 wt % of GnPs enhanced the electrical conduction of the PEDOT:PSS conductive ink from $\sigma \approx 0.8 \times 10^2$ S/m to $\approx 1.8 \times 10^2$ S/m. Moreover, the sensing capability of the device was improved after GnPs addition. Indeed, GnPs enhanced the active surface area of the sample (increasing the surface roughness), and augmented the electron interaction between the sample and ammonia gas.

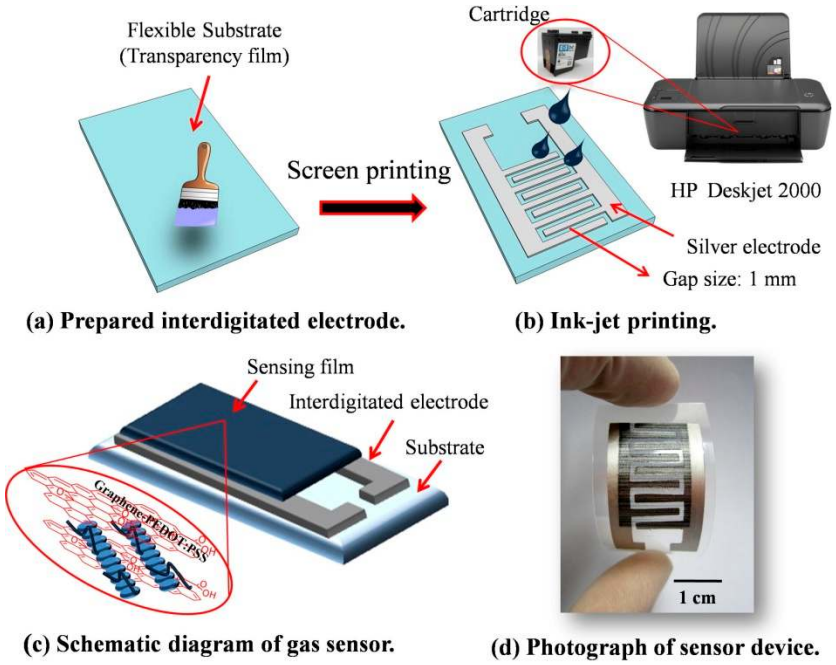

Figure 4. Schematic diagram of the manufacturing process of the ammonia sensor. (**a**,**b**) a silver interdigitated electrode was screen printed on transparent paper. The GnPs-PEDOT:PSS sensing film was deposited trough ink-jet printing; (**c**) schematic of the ammonia gas sensor. (**d**) photo of the obtained device. Reprinted with permission from Organic Electronics 15, 11, 2971–2981. Copyright 2014 Elsevier.

More recently, Huang et al. [57] used a combination of screen printing technology and rolling compression to develop GnPs-based radio frequency flexible antenna. They functionalized paper with the GnPs, obtaining electrical conductivity of 4.3×10^4 S/m. To verify the antenna's flexibility, they measured the reflection coefficient of bended devices, recording almost the same performance as with the un-bent antenna. To perform the described experiments, Huang et al. employed commercially available GnPs-based conductive ink (grade Grat-ink 102E from BGT Materials Ltd., Manchester, UK) which contains graphene nanoflakes, dispersants, and solvents. The described approaches result in flexible and conductive materials with remarkable applications. However, often mechanical durability and electrical features are not balanced [67]. Indeed, the lack of resistance to bend cycles and mechanical stresses limits the range of uses of such electronics materials in applications such

as wearable and motile sensors technologies. Certainly, in the case of GnPs inclusion inside plastics, increasing the filler loading inside the polymer matrices can transform the latter into brittle materials and lead to complications in manufacturing [67].

Mates and collaborators [58] took one step towards the creation of GnPs-based durable materials for flexible electronics. Indeed, they realized a conducting composite coating dispersing GnPs of different sizes inside acrylic paint emulsions. Such composite films were spray casted onto Xerox printing paper, heat-cured, and polished. The adhesion of the conducting layer to the substrates was tested by Taber abrasion and peel tests, displaying remarkable resistance under such mechanical stress. The electrical conductivity reached values of approximately 5×10^2 S/m, and kept the same order of magnitude after 100 cycles of abrasion or peeling. Mates and coworkers also found that GnPs flakes with larger planar dimensions positively affect THz EMI shielding efficiency (see Figure 5). The best results obtained by Mates et al. were obtained by employing commercially available GnPs acquired from Strem Chemicals (typical thickness of 6–8 nm, lateral size of 5, 15 and 25 microns).

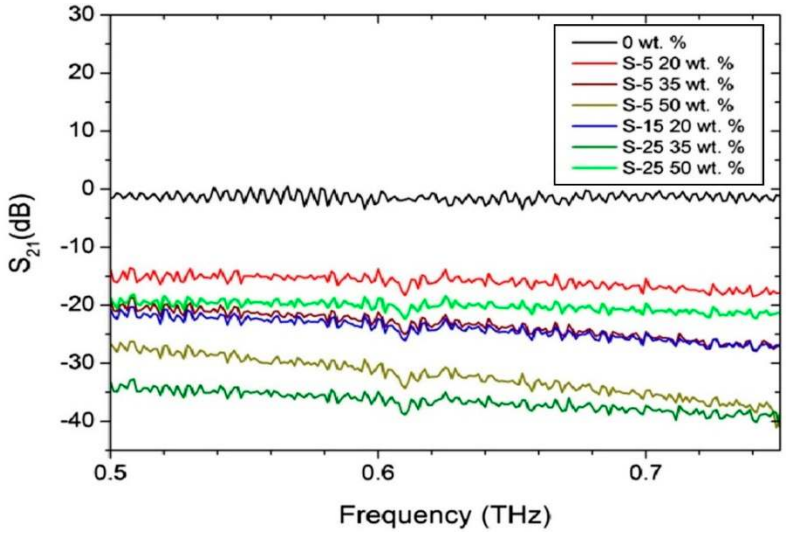

Figure 5. EMI shielding effectiveness (S_{21}) of the GnPs-acrylic paint emulsion as a function of GnPs concentration and type (S-X, where X express the average lateral size of the nanoflakes). The frequency investigated were between 0.5 and 0.75 THz. The highest level of attenuation (≈36 dB) was found for the high-conductivity composites. An all-paint composite (0 wt % GnPs) was also tested as a negative reference. Reprinted with permission from Carbon 87, 163–174. Copyright 2015 Elsevier.

Another step towards reliable GnPs-based flexible electronics was demonstrated in the study of Hyun and coworkers [59]. They started by filtering a graphene dispersion using a PTFE membrane, and used a transfer printing process (a simple pen) to transfer the conductive nanoparticle onto paper. Multiple folding cycles were not sufficient to damage the material's electrical conductivity. Indeed such GnPs-paper composite maintained about 83%/94% of the initial electrical conductivity after 1000 cycles of 180°/−180° folding. Scidà and coworkers [60] designed a GnP-based antenna for near-field communication. This material exhibited significant electrical conductivity, i.e., $\sigma \approx 10^5$ S/m. The GnPs were hot-compressed, forming freestanding GnPs films that were laminated onto polymeric substrates (see Figure 6) or textiles. The performance of the devices was stable after hundreds of thousands of bending cycles at bending radii of 45 and 90 mm. The GnPs employed for this research were supplied by Avanzare (Navarrete La Rioja, España) (product AVA18, D50 = 50 µm).

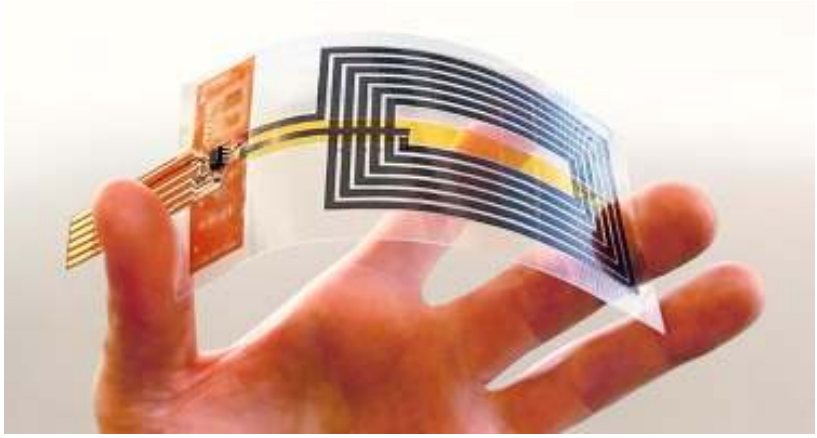

Figure 6. Image of the flexible GnPs-based antenna manufactured on transparent plastic substrate. Reprinted with permission from Materials Today 21, 223–230. Copyright 2018 Elsevier.

Recently, Oh et al. [61] fabricated GnPs-based transparent electrodes for flexible optoelectronics. The nanoflakes were brush coated on PMMA and silver nanowires were sprayed uniformly on top. The entire structure was embedded onto PET or PDMS. With this technique, a sheet resistance of 12 Ω/sq with transmittance of 87.4% was reached. After 10^5 bending cycles, the resistance increased by only the 4%. Such a GnP-based electrode was doped with p-type $AuCl_3$ and Cl_2, and used as the anode in organic light emitting diodes, substituting and performing better under bending and stretching than standard indium thin oxide.

2.2. Environmentally-Friendly Graphene-Based Materials and Devices

Another valuable and important parameter for the electronics of the future will be their sustainability (i.e., the biodegradability of the components and/or the green approaches employed to produce the materials) [68,69]. Indeed, electronic goods production and waste management have become a major issue for environmental pollution [68,69]. A novel method was proposed by our group [43] to fabricate isotropically electrically conductive biodegradable biocomposites based on cellulose and GnPs. It consisted of hot-press impregnation of porous cellulose networks after spray coating the flexible fibrous cellulose substrates with conductive GnPs-based inks. Since such ink was made employing a biodegradable thermoplastic polymer (Mater-Bi®), hot pressing at a temperature higher than the melting of the plastic led to the polymer-GnPs incorporation inside the fibrous network. The resultant green materials exhibited remarkable electrical conduction ($\sigma \approx 10^3$ S/m) and a significant folding stability after severe weight-assisted 180° folding-unfolding cycles at 0 mm bending radius. Such conductive materials were used to fabricate simple circuitry [43], and as a top electrode for organic photovoltaics solar cells [62]. Another green approach developed by our group [63] to obtain reliable bio-based material for foldable electronics was to take advantage of the liquid absorbing properties of pure cellulose. A green conductive ink realized employing methanol and acetic anhydride as solvents, and cellulose acetate and GnPs as solid content, was spray coated onto pure cellulose. The ink thoroughly wet and impregnated the cellulose substrate after deposition, eliminating the need for hot-pressing. This cellulosic-GnPs bionanocomposite exhibited good folding stability and abrasion resistance. Proposed applications were sustainable THz electromagnetic shielding materials and electromyography signal detection (see Figure 7). The GnPs employed by our group for these studies were provided by Directa Plus (grade Ultra g+). For details on the lateral size and thickness of such nanoflakes, see this report [65].

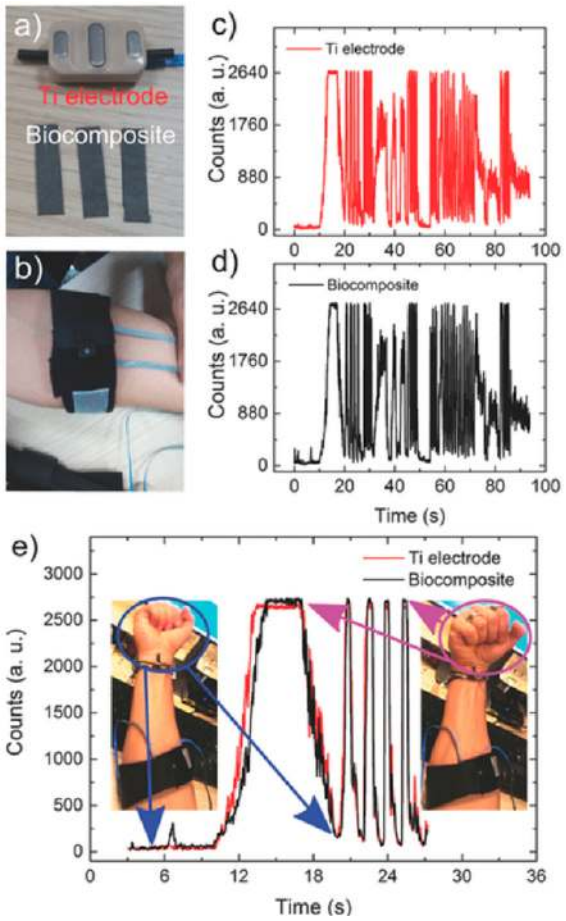

Figure 7. GnPs-cellulose nanocomposite used as electrode for surface electromyography. (**a**) Photograph displaying a standard electromyography titanium electrode (Ti electrode) and the cellulosic biocomposite; (**b**) Photograph showing both electrodes strapped to the arm side by side; (**c**) Signal acquired from the titanium conductor; (**d**) Signal recorded from the biocomposite; (**e**) Superimposed signals from both conductors. The signal rests at zero when the wrist is not flexed (inset on the left). The signal saturates when the wrist if flexed (inset on the right). Reprinted with permission from Advanced Electronic Materials, 2, 11, 1600245. Copyright 2016 Wiley.

Another green nanocomposite for flexible electronics was lately proposed by Liu and collaborators [64]. They added GnPs and cellulose nanofibril into polylactic acid and conductive polypyrrole composite via a green, cost effective method. The addition of GnPs enhanced the electrical conductivity of the biocomposites from 12 to 106 S/m at 10 wt % nanoflakes concentrations. The nanocomposites exhibited also remarkable flexible stability, with only 7.5% deviation after 100 cycles. The GnPs and nanofibril addition also enhanced the mechanical properties of the biocomposite. The nanocomposite was employed as the electrode for flexible supercapacitors.

2.3. Flexible Electronics Outlook

In brief, GnPs have a high potential for flexible electronic devices. EMI shielding, antennas, supercapacitors, and bendable electrodes for solar cells are the most promising applications. The employment of large scalable production processes, together with the industrial availability of GnPs and the high resistance to mechanical stresses (e.g., bending cycles and abrasion), are all encouraging for the large-scale expansion of GnP-based flexible electronics. The large number of work dealing with the functionalization of cellulose and/or the employment of biopolymers and green methods is also promising for the future of sustainable electronics [68,69].

3. Wearable Electronics Based on Graphene Nanoplatelets

Smart textiles are fibrous materials with numerous functionalities and applications compared to common fabrics [70]. It is predicted that the wearable device market will reach US$ 20.6 billion in the current year (2018) [71]. Electrical conductivity is the main promising feature of these garments, because it is highly sought after in fields such as flexible, wearable, and deformable electronics, and for the emerging Internet of Things [71,72]. Miniaturization propelled by nanotechnology allows us to fabricate electronic components, even working on a single fiber [72]. However, direct functionalization of textiles is more often targeted by the incorporation of conductive nanoparticles inside/on fibrous networks [73–76]. Using such an approach, remarkable results were achieved in applications related to generators [77], supercapacitors [78], and electrochemical sensors [79]. Nevertheless, further research is needed to create wearable conductive materials with stable electronic performance under mechanical stress and ambient conditions (e.g., sunlight, air etc.). In particular, wearable electronics require the creation of a new class of materials which are flexible, foldable, and washable, and which, at the same time, maintain a satisfactory level of electrical conductivity [48]. Polymeric nanocomposite materials, due to the intrinsic mechanical properties of polymers and ease of manufacturing, and to the large spectra of properties accessible with different nanoparticles, are suitable for conductive wearable technologies [80].

In this regard, promising approaches are: (1) the functionalization of fabric with Graphene Oxide (GO) [76,81–83], (2) the employment of graphene-based materials to produce conductive fibers [84–86], and (3) the transfer of chemical vapor deposited graphene films onto textiles [87,88]. All these approaches present enhancements compared to metal functionalization [89]. However, some limitations can be identified [89]:

(1) Graphene oxide needs reduction steps, and the obtained sheet resistance is often high (i.e., in the order of thousands of Ω/sq).
(2) Graphene freestanding fibers have remarkable electrical properties, but difficult adaptability to the current garment industry.
(3) Chemical vapor deposition of graphene is expensive, and the transferring procedure of the film is complicated.

Recently, another promising procedure was reported to impart electrical conductivity to industrially produced fabrics through a functionalization based on GnPs. This method has the advantage of being adaptable to several commercially-available materials like cotton and polyesters, and since GnPs are already produced in amounts suitable for the textiles market (hundreds of tons), it is scalable.

For example Woltornist et al. [89] prepared a conductive GnP-infused poly(ethyleneterephthalate) fabric by dip coating and tip sonication in heptane and water. They reached a few kΩ/sq sheet resistances at 15 wt % loadings. Sloma and coauthors [90] fabricated electroluminescent structures on textiles (paper and cotton), employing GnPs as transparent electrodes. They obtained a transmission of 70% of the incoming light, and sheet resistances in the order of 10 kΩ/sq. Tian and collaborators [91] produced a conductive fabric by layer-by-layer deposition of GnPs doped PEDOT:PSS-chitosan on cotton. Such fabrics featured ohmic I-V curves and could achieve an electrical conductivity of $\sigma \approx 0.4$ S/m (see Figure 8a). Furthermore it was resistant to washing cycles, and simple circuitry could be realized, powering up LEDs, as shown in Figure 8b. The fabric also showed remarkable ultraviolet protective ability, i.e., approximately 300-fold higher than the control fabric.

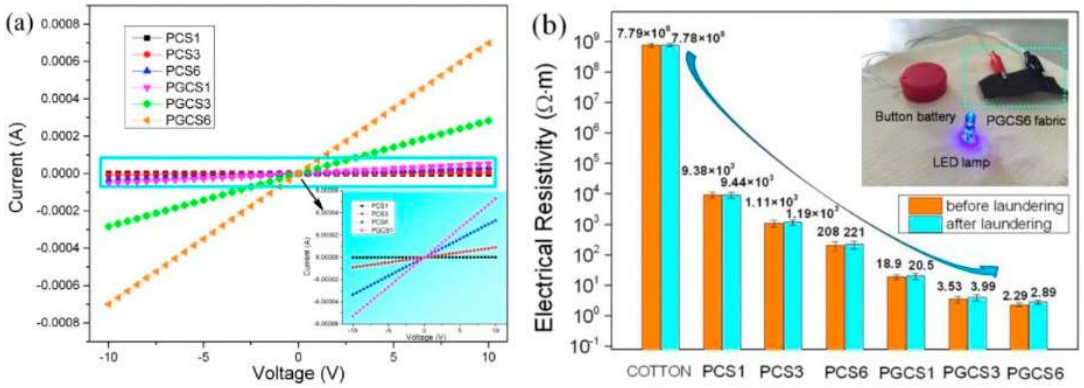

Figure 8. Electrical characteristics of the conductive cotton fabric produced by layer by layer deposition of GnPs doped PEDOT:PSS-chitosan on the textile. (**a**) I–V curves for different specimen labeled as PCSX (PEDOT:PSS and chitosan) and PGCSX (PEDOT:PSS/GnPs and chitosan) were X is the number of layer deposited. For example PCS1 is the sample obtained depositing one thin film of PEDOT:PSS and chitosan; (**b**) Electrical resistivity of control fabric, PCSX and PGCSX fabrics (before and after water laundering 10 times). Reprinted with permission from Carbon 96, 1166–1174. Copyright 2016 Elsevier.

Printing and spraying were also employed in the context of wearable electronics. For example, Skrzetuska et al. [92] screen printed a GnP-carbon nanotubes conductive paste onto cotton. The formulation of the paste was water based, and they were able to reach sheet resistances in the order of a few kΩ/sq. To bind the textile and the conductive nanofillers, they added a cross-linking agent (aliphatic urethane acrylate) to the preparation. Recently, our group [93] fabricated wearable conductive cotton fabric through simple spray procedures. A conductive ink was realized by mixing thermoplastic polyurethane (TPU) and GnPs. Such a dispersion was deposited onto cotton and impregnated through a hot-pressing procedure. The resulting material exhibited sheet resistances ~10 Ω/sq, as shown in Figure 9a. Furthermore, the conductive fabric displayed significant resilience against multiple weight-pressed folding cycles, while folding-induced micro-cracks could be easily healed by repeating the hot-pressing procedure, restoring the initial value of sheet resistance (Figure 9b). The nanocomposite conductivity was unaffected by high humidity conditions and solar irradiation, and was slightly modified by laundry cycles. In our research we used a commercially available GnPs (grade Ultra g+ GnPs, Directa Plus S.P.A.).

Wearable Electronics Outlook

As shown, GnPs have good potential in smart fabric applications. Nevertheless, so far, the highest limitation is the difficulty to bind GnPs to textiles and ensure washing stability and durability. In this prospect, GO is more diffused because, with its oxygen groups, it is simpler to be chemically linked to cotton [76]. However, GnPs are more suitable than GO for applications which need high electrical conductivity. Therefore, smart solutions to effectively bind the nanoplatelets with fabrics will enlarge their potential in wearable and textile electronics, and boost the spread of GnP-based smart garments. The junction of nanoflakes with elastomeric polymer seems to be a suitable approach [93].

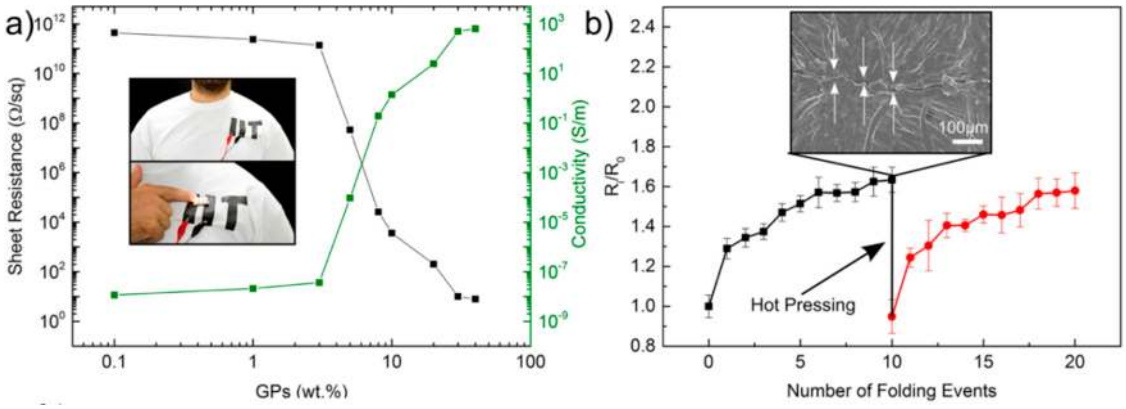

Figure 9. Electrical characteristics of the thermoplastic polyurethane GnPs nanocomposites spray coated on cotton. (**a**) Electrical conductivity and sheet resistance measurements as a function of GnPs concentration with respect to thermoplastic polyurethane. In the inset, a conductive path is spray coated on a t-shirt and used as conductor to light-up LEDs. (**b**) Black line: modifications in the sheet resistance due to weight-pressed 0 mm bending radius folding-unfolding events. The inset displays crack formation after the 10th cycle. Red line: performance after healing the crack by hot-pressing. Reprinted with permission from ACS Appl. Mater. Interfaces 9, 16, 13825–13830. Copyright 2017 American Chemical Society.

4. Graphene Nanoplatelets for Strain Sensors and Stretchable Electronics

The field of wearable and stretchable electronics pushes towards unusual material arrangements to design circuitries on curvilinear and deformable structures/organisms, and fabricate soft electrical devices and sensors [71,94–97]. The junction of a pliable and elastomeric material with a conductive nanomaterial is a favorable approach to build compliant nanocomposites for electronics [98–100]. Sensor technologies exploit conductivity and capacitance fluctuations recorded when such nanocomposites are deformed (stretched, wrapped, or compressed). These variations are used as a feedback mechanism for devices like strain, pressure, and tactile sensors [101–103]. Typically, with an external stimuli (often mechanical), conductive nanofillers inside the matrix are separated apart or connected further, changing the material's electrical features.

Following such approaches, flexible and stretchable GnP-based sensors were investigated and designed in the past years (see Table 2) [48].

Table 2. Smart Sensors GnPs-based. Gauge factor is defined as the ratio between electrical resistance change and mechanical strain.

Type of Sample	Manufacturing Techniques	Type of Sensor	Characteristics	Reference
GnPs on PET	Spray coating	Piezoresistive Strain Sensor	Gauge factor 150	[104]
GnPs or CnFs on nitrile rubber	Spray coating	Stretchable Tactile Sensor	Sensitivity 0.03 N	[105]
GnPs-PEDOT:PSS on cotton	Spray Coating	Piezoresistive Strain Sensor	Gauge factor 5	[106]
GnPs inclusion in epoxy resins	Solution processing	Piezoresistive Strain Sensor	Gauge Factor 750	[107,108]
GnPs inside PDMS	Solution processing and molding	Piezoresistive Strain Sensor	Gauge factor 230	[109]
GnPs inside Silly Putty	Solvent mixing	Piezoresistive Strain Sensor	Gauge factor > 500	[110]
TPU-GnPs nanocomposite	Solvent Mixing	Piezoresistive Strain Sensor	Adjustable electrical properties	[111]
GnPs-CnTs inside PDMS	Screen Printing	Piezoresistive Strain Sensor	Gauge factor 100	[112]
GnPs-CnT dispersed in PMMA/PVDF	Screen printing on plastic	Pressure Sensor		[113]
Glass fiber coated with GnPs	Dip coating	Piezoresistive Strain Sensor	Gauge Factor 16,000	[114,115]
Textiles functionalized with GnPs-poly(vinyl alcohol)	Dip Coating layer by layer assembly	Piezoresistive Strain Sensor	Gauge factor 1800	[116]
GnPs on medical tape and embedded in PDMS	Press and molding	Piezoresistive Strain Sensor	Gauge factor 110	[117]
CnTs grow on GnPs inside PDMS	Mechanical Mixing	Piezoresistive Strain Sensor	Gauge factor 1000	[118]
GnPs-PDMS nanocomposites	Layer by layer spin coating	Capacitive Strain Sensor	Linear capacity variation	[119]
GnPs-PDMS foam	Direct template	Pressure Sensor	Sensitivity 0.23 kPa^{-1}	[120]

Strain sensing is crucial for the advances in smart robots, human/structure health monitoring, and human-machine interactions [108,117,121,122]. Indeed, the strain gauge market surpassed 4.5 billion $ in 2013, and is growing constantly [104]. The most important parameter for strain sensing is the gauge factor. This parameter is defined as $(\Delta R/R)/(\Delta L/L)$, where $(\Delta R/R)$ is the relative change in electrical resistance (R) obtained under material elongation, and $(\Delta L/L)$ is the applied strain. Graphene-based materials have shown gauge factors among the highest ever reported [103]. Two-dimensional nanoflakes usually show a piezoresisitivity one order of magnitude higher than that of nanowires, since their electrical percolation network is largely susceptible to geometrical changes and discontinuities [123]. Furthermore, carbon-based fillers can expand the utilization of strain sensors, enhancing their elongation range from a few to several hundred percent stretches [122,124].

Different approaches were employed to realize GnPs-based strain sensors. The most commonly-used feedback mechanism is based on stretch-induced electrical resistance changes (piezoresistivity). Hempel et al. [104] designed strain gauges by simply spraying pristine GnPs thin film on plastic PET substrates. Changing the spray parameters, they were able to control the coating morphology and decrease the film resistance by varying the amount of deposited dispersion. The gauge factor was stable over 4000 strain cycles, and exceeded 150. The electrical percolation behavior of the system under stretch was in good agreement with a model simulating a link between randomly-oriented conductive disks.

4.1. PDMS and Graphene Nanoplatelets for Strain Sensing

A widespread material for strain sensors is polydimethylsiloxane (PDMS), due to its flexibility, stretchability and ease of manufacturing [125–130]. PDMS-based strain sensors were also investigated coupled with GnPs. For example, Wang and collaborators [109] developed GnPs-PDMS composites by simple sonication and molding processes. This device reached gauge factors of approximately 230 at a GnPs concentration of around 8 vol %, and within a strain of 2%. Shi and collaborators [117] produced an electrically conductive and stretchable film by mechanically pressing GnPs onto a medical tape and embedding the structure inside PDMS. The manufacturing was low-cost and fast (in the order of one minute), and therefore, large-scalable. The obtained sensor was reliable over 1000 stretch-release cycles, exhibited a time of response of less than 50 ms, and a gauge factor of approximately 110. Moreover their sensor showed sensitivity to low mechanical strains. Indeed, it could detect minuscule movements from a cricket, and air vibration caused by mobile phone speakers, as shown in Figure 10.

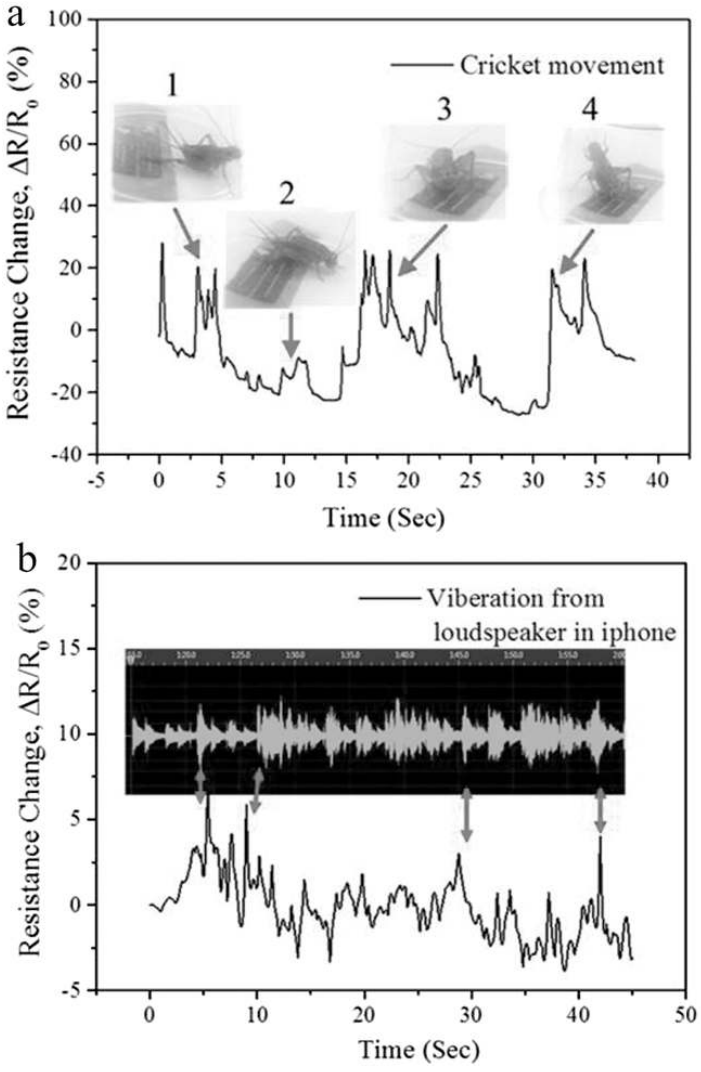

Figure 10. Performance of the deformation sensor obtained pressing GnPs on a medical tape and embedding such structure inside PDMS. The sensor was employed as tiny movements and sound signal detector. (**a**) Signal generated by the footstep of a field cricket moving on the sensor and (**b**) recognition of music signal from an iPhone speaker, with inset being audio signal. Reprinted with permission from Advanced Functional Materials. Copyright 2016 Wiley.

Another PDMS and GnPs composite for strain sensing was investigated by Lee and collaborators [131]. They used layer by layer assembly to create controlled geometries of GnPs on the elastomeric substrates. Such devices can monitor subtle human movements.

The synergic properties of GnPs and carbon nanotubes are convenient to design PDMS-based strain sensors. For example, Lee et al. [112] screen printed a biocompatible gauge device employing multilayer graphene nanoflakes and multiwall carbon nanotubes (MWCNT). The gauge factor changed from 22 (for 12.5 wt % GnPs inclusion) to 100 for concentrations near the percolation threshold (i.e., 1.5 wt % GnPs and 3.5 wt % MWCNT blend). The authors attribute such behavior to the large contribution of electron tunneling at nanofiller loads close to the percolation threshold; with stretch, the distance between nanofiller units augment, however, still permitting tunneling conductivity. For higher filler loads, the mechanism of conductivity is mostly determined by direct contacts that are slightly affected by strain compared to tunneling electrons. More recently, Zhao and collaborators [118] used catalyst chemical vapor deposition approaches to grow nanotube forests on both sides of GnPs nanoplatelets. The nanoflakes-nanowires filler was mechanical mixed with PDMS, achieving percolation threshold at 0.64 vol %. At 0.75 vol % concentration, they reached a gauge factor in the order of 1000. Such sensors are able to sense and even distinguish between tiny finger motions, as shown in Figure 11. Furthermore, the nanocomposites were also used as compression sensors, reaching pressure sensitivity of 0.6 kPa^{-1}.

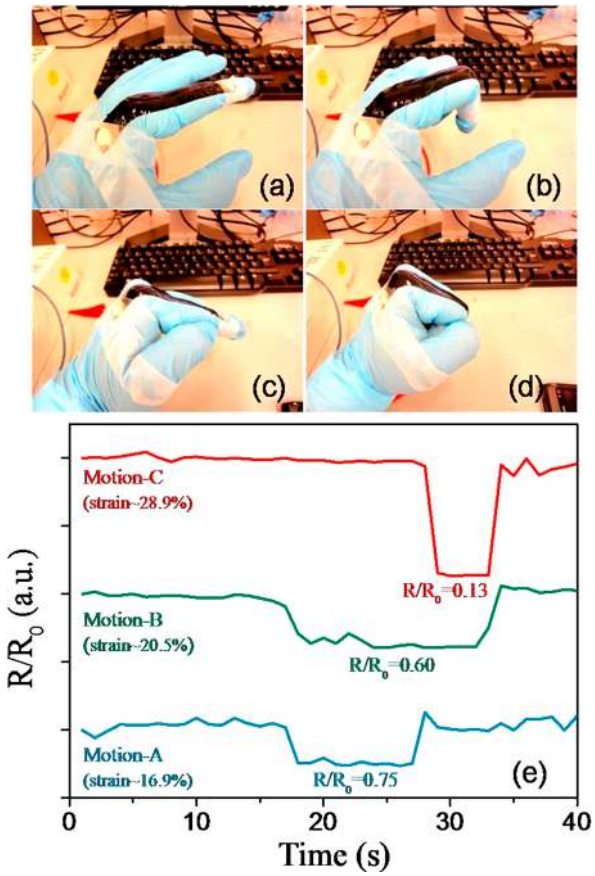

Figure 11. Nanoflakes-nanotubes PDMS composite film glued on rubber gloves and serving as finger motion detector. (**a**) Photograph of the relaxed state of the finger; (**b**–**d**) are photographs of second and third joint and clenching motions respectively; (**e**) Resistance changes for each independent movement. Reprinted with permission from ACS Appl. Mater. Interfaces 7, 9652–9659. Copyright 2015 American Chemical Society.

4.2. Other Approaches for Graphene Nanoplatelets Based Strain Sensing

Apart from PDMS, other rubbery materials are also candidates for possible implementation for strain sensing. For example, Boland and coauthors [110] used a highly viscoelastic, lightly cross-linked silicone polymer (trademark name Silly-Putty®) mixed with GnPs to design a material that can monitor impact, pressure, and deformation. Its electrical resistance augmented linearly when stretched below 1%, and surprisingly decreased, even below its initial value for elongations between 1% and 10%. Such a trend is unique considering the monotonic increases of resistance usually observed with stretch. Silly-Putty-GnPs nanocomposites exhibit gauge factors of around 500 at 6.8 vol % of nanofillers. Such device can measure blood pressure, pulse rate, and even the footstep impact associated with spiders. The GnPs (Lateral size $\approx$ 500 nm, thickness $\approx$ 20 layers) employed for this work were prepared by ultrasonic tip-sonication of graphite (Branwell, Graphite Grade RFL 99.5) in NMP. These GnPs were then dispersed in chloroform after NMP drying. Recently, our group [111] showed that electrical conductivity of TPU-GnPs nanocomposites can be tuned and improved by repeated stretching cycles, without exceeding 20% of the maximum strain. A decrease of up to 60% in electrical resistance was measured after 1000 stretch-release cycles. We discovered that the described changes were caused by stretch-induced redistribution of the GnPs within the polymer matrix. Such TPU-GnPs nanocomposites can be used for strain sensing applications after stretch-induced electrical feature optimization. The rearrangement of the disposition of nanoflakes inside TPU was noted also by Liu and collaborators with single layer graphene [132]. Wearable and stretchable textiles are ubiquitous. Another common strategy for strain sensing is the functionalization of such fabrics with conductive materials. For example, Zahid and collaborators [106] obtained a conductive ($\approx$200 S/m) textile functionalizing cotton through a simple spray of PEDOT:PSS-GnPs dispersions. The material exhibited strain sensing capabilities, with a gauge factor of approximately 5 at strain of 5% and 10%. It could resist repeated washing and bending events, thereby ensuring possible commercialization.

The combination of high sensitivity to tiny deformation and broad sensing range is often unusual in the field of strain sensors [133]. In such a context, promising results were obtained by Park et al. [116], who reported on the fabrication of stretchable yarns realized through simple layer-by-layer assembly. In particular, different yarns (rubbery, nylon-rubbery and wool) were immersed first in a poly(vinyl alcohol) solution, and, when dry, in a GnPs dispersion. All these fabrics maintained a remarkable stretchability (see Figure 12). When needed, a PDMS coating was used to prevent GnP detachment during stretch. Depending on the fiber used, different performances were achieved. Indeed, the highly sensitive rubbery sensors exhibited a gauge factor of $\approx$1800 and a maximum stretchability of around 100%, the nylon-rubbery device led to a gauge factor of 1.4 and a maximum elongation of 150%, and the wool-based sensor displayed an atypical negative gauge factor of -0.1 with a maximum stretch of the 50% of the initial length. These performances are suitable for monitoring a wide range of body movements depending on the fiber employed, from tiny breathing to finger-bending.

Moriche et al. [114] investigated the use of fabric-like material coupled with GnPs for strain sensing applications. They dip coated glass fiber with conductive nanoflakes, observing that this coating was more effective when GnPs were NH_2 functionalized. Also, electrical conductivity and strain sensing were strongly enhanced when GnPs were doped with nitrogen. Such GnP textiles exhibited an exponential increase in resistance with stretch, reaching gauge factors in the order of 16,000. Additionally, functionalized fibers attached on nitrile gloves were able to monitor single finger movements. Strain sensing can be also performed by monitoring the electrical capacity variation when a material is mechanically deformed. Filippidou et al. [119] realized a deformable PDMS-GnPs plain capacitor. They used a GnP-PDMS composite as the soft electrode and pure PDMS as the elastic dielectric. The capacitor was manufactured simply by a layer-by-layer spin coating technique. The sensor was tested for small strain measurements in the order of 0.2%, showing a linear variation of capacity with stretch.

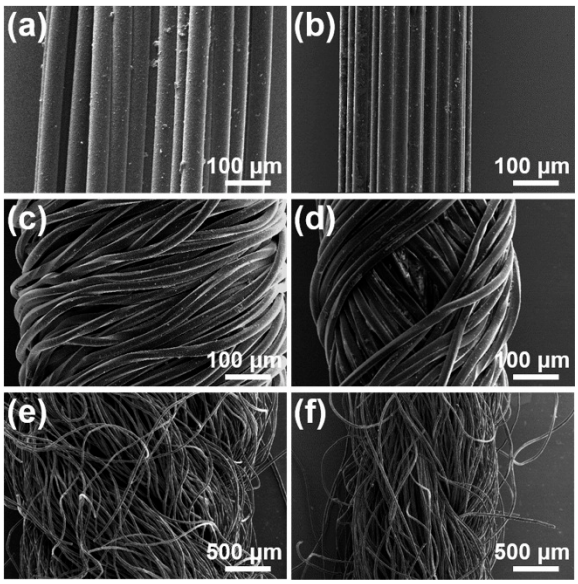

Figure 12. Stretchable and conductive yarns realized through simple layer by layer assembly on different elastomeric textiles. (**a**,**c**,**e**) Scanning electron microscope image of the GnPs strain sensors realized with rubber, nylon-rubber and wool fibers, respectively; (**b**,**d**,**f**) the same textile stretched (100%, 100% and 50% respectively). Reprinted with permission from ACS Appl. Mater. Interfaces 7, 11, 6317–6324. Copyright 2015 American Chemical Society.

4.3. Graphene Nanoplatelets Based Structural Health Monitoring

Structural health monitoring (SHM) is a specific strain-sensing application which needs extremely high sensitivity to minute structural changes [134]. It was thoroughly investigated to enhance the safety of buildings and monitor the stability of structures in real-time, enhancing public security. Due to the high gauge factor, GnP-based nanocomposites are adequate for this purpose. Indeed, recently, researchers have focused on such devices. For example, Moriche and collaborators [107] added GnPs to an epoxy resin used for aeronautic applications. Nanocomposites with nanofiller contents of around the electrical percolation threshold displayed high gauge factors (≈750) at strains inferior to 1%. They discovered that the dominant strain sensing mechanism was based on changes on the distance between nanoflakes. The resultant exponential electrical change was explained with a diminished tunnel effect. Increasing the amount of GnPs, the direct contact mechanism dominated, and the electrical response with stretch became linear. They were able to discriminate between structural changes due to tensile or flexural stress. They also discovered that such modified epoxy resin-GnPs present no hysteresis during 50 cycles of loading-unloading in flexural test conditions, demonstrating the reversibility of the SHM mechanism in the plastic deformation regime [108]. Recently, the same group [115] performed a study on SHM materials obtained by combining NH_2 functionalized GnPs, epoxy resins, and glass fiber. The experiments performed in this section were performed with commercially available GnPs provided by XGScience (nominal thickness 6–8 nm and lateral size 25 microns).

4.4. Pressure Sensors

In addition to strain sensors and SHM, Rinaldi et al. [120], advanced flexible and compressible pressure sensors functionalizing PDMS foams with GnP dispersions. The manufacture of PDMS foam was achieved following the direct template technique, which implicates the replication of the inverse assembly of a preformed leachable prototype (see Figure 13 for details). In particular, they discovered that such device exhibited a linear regime for pressures <10 kPa, while at higher pressures, the electrical conductivity increase with higher steep (maximum 70 kPa, 800% resistance change). The sensitivity was of 0.23 kPa^{-1}.

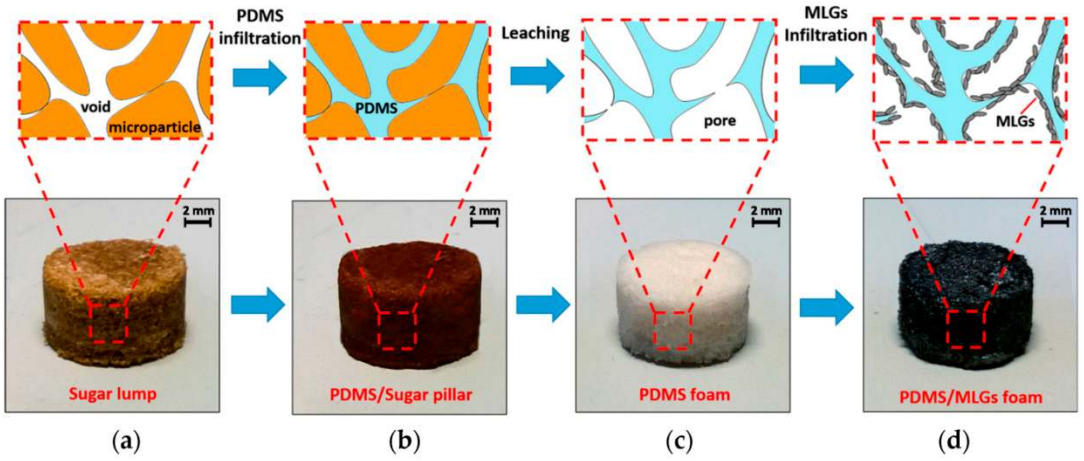

Figure 13. Manufacture steps for the fabrication of PDMS-GnPs foams. (**a**) Sugar template; (**b**) PDMS infiltrated sugar template; (**c**) Sample after the sugar removal; (**d**) PDMS/Multilayer graphene (MLGS) foam resulting after nanoflakes infiltration. Reprinted with permission from Sensor 16, 12, 2148. Copyright 2016 MDPI.

Janczak and collaborators [113] screen printed GnPs and carbon nanotubes dispersed in PMMA or PVDF on flexible substrates. Such conductive composites were employed as the active layer in pressure sensors. The sensitivity of the sensor was proportional to the sheet resistance of the material.

4.5. Capacitive Sensors for Tactile Sensing

There are applications in stretchable electronics which require materials with stable electrical features under constant elongation conditions, such as electronic skin and elongating touch sensors. One of the methodologies employed to build artificial electronic skins is deformable capacitors that can identify touch-induced pressure, shear, and torsion [135]. Ensuring the functionality of such capacitive devices under mechanical stress (bent and even more stretched exceeding 100%) is challenging [136].

Our group [105] recently reported the fabrication of a durable stretchable haptic capacitive sensor using nitrile rubber as template. A conductive elastomeric polymer dispersion containing GnPs or carbon nanofibers (CnFs) was spray coated onto both sides of a nitrile rubber piece, obtaining a parallel-plate capacitive touch sensor. The conductive spray, either GnP- or CnF-based, reached satisfying sheet resistance levels, i.e., ≈10 Ω/sq. The GnP-based conducting electrodes formed cracks before 60% elongation, while the conducting electrodes based on CnFs sustained their conductivity at up to 100% strain level. However, both electrodes were adaptable and trustworthy, considering the motility and elongation level of human junctures (≈20–40% strain). Remarkably, structural deterioration due to cyclic stretch-release events could be healed as a consequence of a straightforward heat gun annealing process. We also demonstrated the haptic sensing characteristics of an elongating capacitive device by wrapping it around the fingertip of a robotic hand. Tactile forces could be detected without difficulty by the device over curvilinear surfaces or under elongation (see Figure 14). The experiments performed in this section were performed with Ultra g+ commercially available GnPs obtained by Directa Plus S.P.A.

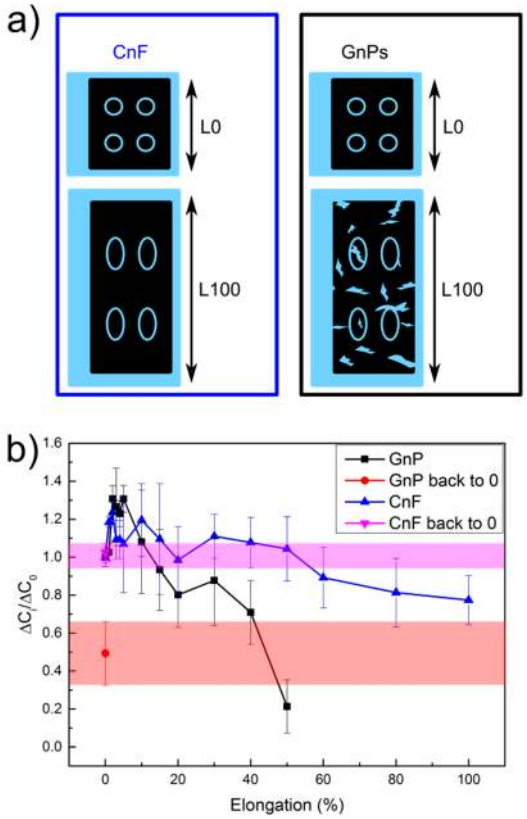

Figure 14. Haptic sensor functionality under elongation of elastomeric conductive inks sprayed on both sides of nitrile glove pieces. (**a**) Graphic representation of the CnF- and GnP-based tactile sensor at 0% elongation (L0) and at 100% stretch (L100); (**b**) device performances at consecutive elongation steps. ΔC_i and ΔC_0 represent the capacity deviation with touch under elongation and at 0% stretch, respectively. Reprinted with permission from Advanced Science 5, 2, 1700587. Copyright 2017 Wiley.

4.6. Smart Sensing Outlook

In summary, GnP-based smart sensors have been extensively investigated to date and are already considered mature for large-scale production. In particular, strain sensing is a more promising application, considering the high gauge factor obtained using GnPs. Such nanoflakes are an excellent candidate for applications which demand high sensitivity to tiny deformations (like structural and health parameter monitoring), broad sensing range, or a combination of the two. To date, PDMS-GnPs strain sensors are the most studied. Another promising approach for stretch sensing is functionalizing textiles with conductive materials to obtain fibrous strain sensors. So far, piezoresistive devices were investigated much more, but some examples using capacitive feedback mechanism are present in the literature. GnP-based stretchable and deformable sensors were also employed for pressure sensing and robotic tactile sensing, obtaining remarkable results.

5. Advanced Reinforced Graphene Nanoplatelet-Based Bio-Nanocomposites

Graphene-based reinforced nanocomposites showed a prominent role in the field of advanced materials [137–141]. The outstanding mechanical properties of single layer graphene, GnPs and GO, led to a new generation of improved plastic-based structural materials [17,142,143]. For example, these 2D carbon-based fillers are attractive for the realization of next generation sporting goods [144], concrete [145], anti-corrosion coatings [146], automotive lightweight components [147], structural elements in aerospace [148], and wind turbine designs [149]. In particular, GnP powder is already produced at large scales and at a low price compared with single-layer graphene, and as such, is more appealing for the composite market [150]. Furthermore, GnPs were already selected as

nanofillers for toughening polymeric materials, since they are strong, and present lower defect concentrations compared to GOs [151]. GnPs integrate the excellent mechanical characteristics of carbon nanotubes with the multi-flakes structure of clays, which can impart superior structural property improvements [150]. Indeed, they were shown to perform significantly better than these nanofillers in enhancing the mechanical properties of nanocomposites such as tensile strength, elastic modulus, fracture toughness, fracture energy, and resistance to fatigue and crack growth [65,152], due to their higher compatibility with polymers matrix [153].

To obtain an effective reinforcement, a crucial requirement is the homogeneous dispersion of the flake-like filler inside the polymer matrix [17,24,143,154–156], as schematically shown in Figure 15a. However, such conditions are necessary but not sufficient. Indeed, also flake dimensions (lateral size and thickness), alignment, and chemical interaction with the matrix (see Figure 15b) need to be taken into account [24,154,156–158]. Furthermore, a recent paper by Papageorgiou et al. [159] investigates in depth the mutual interaction between graphene-based materials and the hosting matrix. Through the examination of hundreds of papers on graphene composites, they demonstrated that the fillers modulus is dependent on the polymer matrix. In particular, the GnPs modulus is larger when the filler concentrations are reasonably low and the matrix is more rigid. This implies that the common hypothesis that the nanoflake modulus is independent of the matrix is not correct.

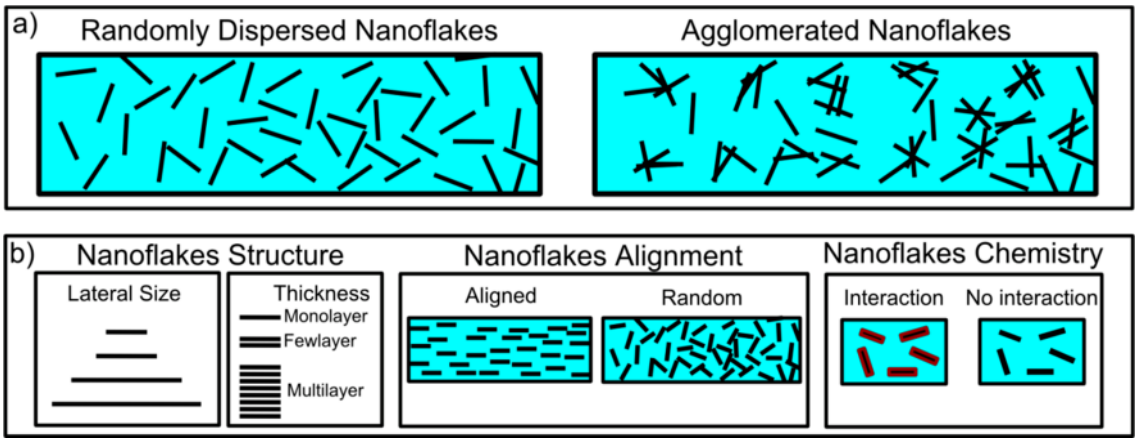

Figure 15. Important parameters for polymer reinforcement by nanoflake inclusions. (**a**) Schematic of homogeneously dispersed and agglomerated filler inside a polymer matrix. Agglomerations enhance crack propagation; (**b**) Schematic of additional significant parameter for effective reinforcement of plastics with graphene based nanofillers: nanoflake structure, alignment, and chemical interaction with the matrix.

Many works have been published so far dealing with the incorporation of graphene, graphene oxide or GnPs inside traditional synthetic and long-lasting plastics. Several reviews are already available on these topics [17,20,21,23,28,137–141,144,153]. In contrast, reviews centered on the reinforcement of bioplastics with graphene-based materials are still rare [160].

Biopolymers are biodegradable; thus, they contribute only slightly to environmental pollution [161,162]. They are constantly gaining interest, considering that they could gradually substitute oil-based, polluting, synthetic polymers [163–165]. Nevertheless, a broad spread-out of these green plastics is often limited, taking into account their poor mechanical properties [162–164]. Therefore, the incorporation of nano-sized reinforcements in bio-polymeric matrixes is emerging as a strategy to improve the performance deficiency of the bioplastics, and obtain characteristics comparable with the traditional long-lasting ones [163,164,166,167]. As such, the inclusion inside biodegradable matrixes of different nanofillers, such as nanostructured metals, multilayered silicates, silica nanoparticles, and carbon nanomaterial were extensively investigated [163,164,166–168]. Single-layer graphene and GO were used coupled with biopolymers, and two reviews were written

on this topic [167,169]. In contrast, to the best of our knowledge, there is not a systematic review dedicated to GnP-reinforced bioplastics, although their potential in this field is steadily growing (see Table 3) [167].

Table 3. Biocomposite GnPs reinforced. The Young modulus is named E_g, the tensile strenght T_s and the elongation at break S_g. These properties are expressed in percent increment. "=" means unchanged.

Matrix	Manufacturing Techniques	E_g	T_s	S_g	Comment	Reference
BioFlex®	Melt Blending	40%	N/A	N/A	at 5wt % filler	[166]
PLA	Melt Blending	12	20	16	0.25 wt % filler. GnPs inside PLA did not affect human fibroblasts morphology and metabolic activity	[170]
PLA or BioFlex®	Melt Blending	40	=	=	5 wt % filler. GnP affected release of ciprofloxacin without preventing the antimicrobial activity.	[162,171]
PLA plasticized with palm oil Pla/Poly(ethylene Glycol)/palm oil	Melt Blending	N/A	27	60	0.3 wt %. Increased antibacterial properties	[172] [173] [174]
PLA	Melt Mixing	200	N/A	N/A	3 wt %	[175,176]
PLA	Melt compounding	Large 24 Small 10	N/A	N/A	5 wt % Study on the effect of GnPs size on PLA mechanical properties	[177]
PLA	Solution Processing Melt Blending	GO 115% GnPs 156%	N/A	N/A	0.4 wt % GO vs. GnPs	[178] [179]
PCL	Solution processing	12	N/A	12	0.5 wt %	[180]
PLA Mater-bi	Solution Processing and hot pressing	200	N/A	N/A	Effect of few layer graphene vs. GnPs on E_g of both biopolyesters. For comparison other 2D and 3D nanoscale fillers were employed	[65]
Chitosan-tapioca starch	Solution processing	N/A	40	N/A	0.8 wt %	[181]
Regenerated Cellulose	Solution processing	34	56	N/A	3 wt %	[182]
Polyvinyl alcohol	Solution processing	60	40		0.5 wt %	[183]

5.1. Graphene Nanoplatelets Reinforced Polyesters

In particular, polyester bioplastics produced on a large scale, such as poly-lactic acid (PLA), could become more commonplace if their mechanical properties are improved [165]. Indeed, many works deal with the reinforcement of such biopolymers with GnPs [162,164]. For example Botta et al. [166] melt compounded PLA-copolyester biopolymer (BioFlex®) with GnPs, improving the biopolymer's Young or elastic modulus (E_g). They added 1 and 5 wt % GnPs nanofillers into the matrix, increasing E_g of approximately the 40% in the best case. In contrast, the elongation at break and the tensile stress were decreased.

Gonçalves and coauthors [170] melt blended PLA with GnPs. They added different GnP loads (0.1–0.5 wt %), obtaining the maximum mechanical performances (20% increase in tensile stretch, 12% increase of E_g, and 16% increase in toughness) at 0.25 GnPs wt %. They also discovered that the inclusion of GnPs inside PLA did not affect human fibroblasts morphology and metabolic activity at the surface of the samples. These results were obtained with a commercially-available GnPs (XG Science Inc., Lansing, MI, USA, xGnP®, grade C, thickness 10–20 nm, lateral size 1–2 µm). Scaffaro and coworkers modified a PLA matrix with ciprofloxacin and GnPs to obtain biopolymer nanocomposites with antimicrobial properties [171]. GnPs were added at a load of 5 wt %, increasing E_g of the 40%. The elongation at break and tensile strength were almost unchanged. These results can be attributed to the good dispersion level of GnPs achieved during compounding. The incorporation of GnP affected the release of ciprofloxacin without preventing the antimicrobial activity of the obtained materials

(see Figure 16). Scaffaro and coauthors [162] obtained similar results with BioFlex® as polymer matrix. Scaffaro and coauthors employed a commercially-available GnPs from XG Science Inc. (grade C750, thickness lower than 2 nm, lateral size 1–2 μm).

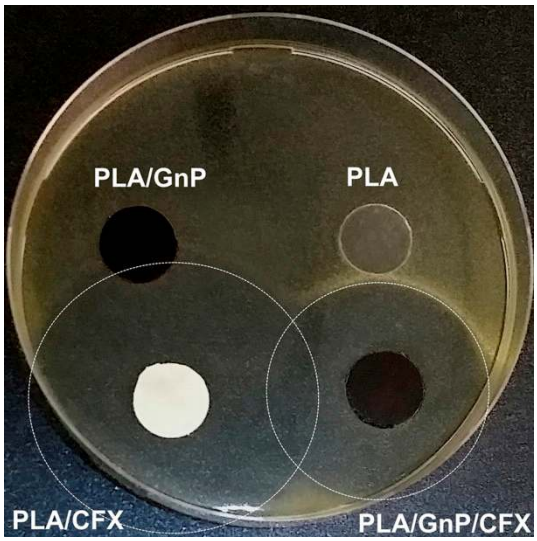

Figure 16. PLA-GnPs-ciprofloxacin composites and their antimicrobial release. Agar diffusion tests were performed with the purpose of investigating if the incorporation of ciprofloxacin inside the PLA specimens was conferring antimicrobial activity to the manufactured films. As bacterium, Scaffaro and coauthors selected *M. luteus*. Both pristine PLA and PLA/GnP displayed no antibacterial properties. In contrast, large bacterial growth inhibition halos were detected near both films, including ciprofloxacin. The presence of GnP led to a reduction of the inhibition zone; therefore, nanoflakes influenced not only the mechanical properties (see text), but also the ciprofloxacin release of the films. Reprinted with permission from Composite part B: Engineering 109, 138–146. Copyright 2017 Elsevier.

Chieng et al. [172] incorporated GnPs inside PLA plasticized with palm oil. With 0.3 wt % nanoflakes melt mixed inside the biopolymer matrix, they were able to increase by approximately 27% and 60% the tensile strength and E_g, respectively. GnPs also decreased the glass transition temperature of the polymer matrix. Similar works always by Chieng et al. were performed mixing PLA, Poly (ethylene glycol), palm oil and GnPs, obtaining similar mechanical improvement [173], and increasing the nanocomposite's antibacterial properties [174]. Other works dealing with melt-mixing inclusion of GnPs inside PLA were published by Narimissa et al. [175,176]. Recently, Gao and coauthors [177] performed a study on the effect of GnP size on the mechanical properties of PLA composites. They used two different commercially available GnPs with lateral sizes of 15 and 1 μm, named large and small, respectively. It was observed that 5 wt % concentrations of the large GnPs augmented E_g by 24%, while the small nanoflakes increased the elastic modulus by 10% at the same concentration. The obtained biocomposites were also electrically conductive, showing a lower percolation threshold for the large GnPs (7 wt % filler loading) compared with the small (13 wt % GnPs concentration).

Other works compare the performance of graphene platelets and graphene oxide inside PLA. For example, Pinto and coauthors [178] reinforced thin films of PLA biopolymer with either GnPs or GO. They used solution processing procedures to fabricate the biopolymers. Both nanoflakes had an optimized load identified at about 0.4 wt % (see Figure 17). In these conditions, GnPs increased E_g by 156% and yield strength by 129%. GO produced similar improvements. Additionally, permeability to nitrogen and oxygen diminished three and four times in films loaded with GO or GnP, respectively. Similar results were achieved by Chieng et al. in this work [179], but by employing melt blending as the production method. In this work [184] Pinto et al. also tested the biocompatibility of reinforced PLA-GnPs and PLA-GO composite materials, finding that low concentrations of graphene-based filler

can be safely incorporated, improving their mechanical properties. More details on graphene-based material biocompatibility can be found in another paper [185] by Pinto and coworker.

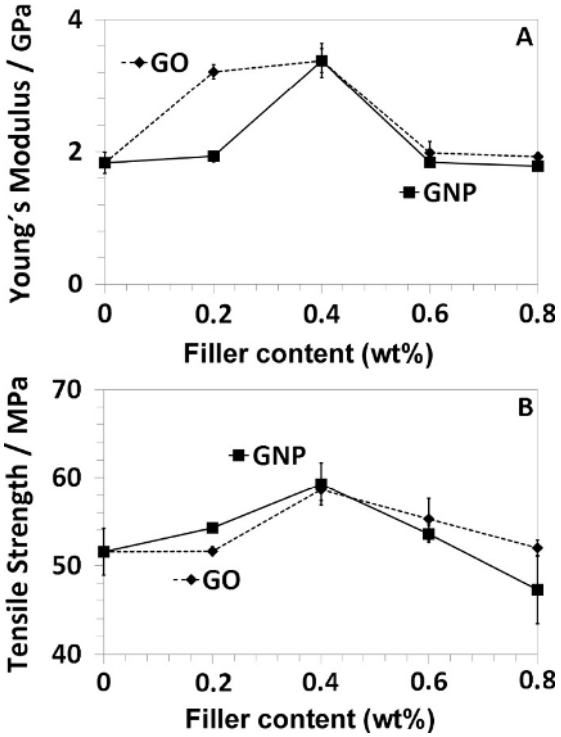

Figure 17. Variation of the Young's Modulus and tensile strength as a function of the nanofiller content of GnPs or GO included inside PLA. Both graphene-based nanofillers increase the mechanical performance of the polymer matrix at low wt % inclusion. Reprinted with permission from Polymer International 62, 1, 33–40. Copyright 2012 Wiley.

Polycaprolactone (PCL), another heavily employed bio-polyester, was coupled with GnPs to enhance its mechanical properties. Wang et al. [180] modified GnPs in water with poly(sodium 4-styrenesulfonate), and compounded such dispersion with PCL. At the best GnP concentration (0.5 wt %), they were able to enhance both the Young modulus and the elongation at a break of approximately the 12%. At 1 wt % GnPs loadings, agglomeration started and the tensile strength and elongation at break reduced considerably. The addition of GnPs augmented notably also the crystallization kinetics. Indeed, only 0.05 wt % nanoflake inclusion triggered a nearly 6 times improvement in crystallization rate.

PLA and Mater-bi® (a blend of PCL and starch) were reinforced with GnPs in our recent work [65]. These two bio-polyesters were mixed with various types of few layer graphene (FLG) and commercially available GnPs. Free standing biocomposites were manufactured by solvent casting and hot-pressing. Exhaustive mechanical measurements were conducted in order to study the effect of FLGs and GnPs thickness and lateral size on the elastic modulus of both polymers. For comparison purposes, other 2D and 3D nanoscale fillers like iron oxides (see Figure 18), clay, and carbon black were used. Under solvent casting conditions (randomly oriented nanoflakes in the polymer matrix), FLG and GnPs did not perform better compared to other model fillers in increasing the elastic modulus of Mater-bi®. On the other hand, both FLGs and large and thick commercially available GnPs increased the elastic moduli of PLA biocomposites more than other 2D and 3D fillers. In the case of hot-pressing induced alignment of the 2D flakes within the polymer matrices, large, many-layer GnPs induced better elastic moduli enhancement compared to FLGs and other 2D and 3D fillers. In particular, GnPs improved the Young Modulus of the Mater-Bi® matrix of the 200%, while PLA enhanced its modulus by 35%. A theoretical model described in the paper is in good agreement with the experimental findings. The

highest Young Modulus improvements were achieved with commercially available GnPs from Strem Chemical and Directa Plus S.P.A. For details see this report [65].

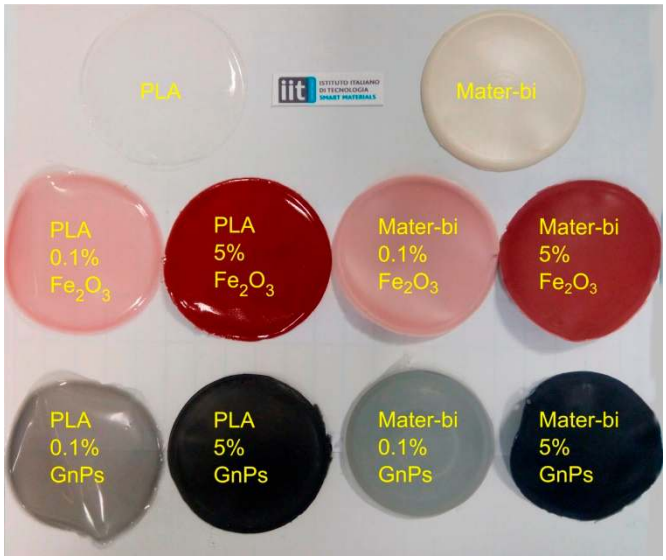

Figure 18. Photograph of different biocomposite films from PLA and Mater-Bi® biopolymers. Whitish and transparent films featured on the top are the pure Mater-bi and PLA matrices. Red films contain Iron Oxides and grey composites include commercially available GnPs. Reprinted with permission from Carbon 109, 331–339. Copyright 2016 Elsevier.

5.2. Reinforcement of Natural Polymer

Apart from bio-polyesters, other biopolymers were also reinforced with GnPs. Ashori et al. [181] included GnPs in chitosan-tapioca starch biocomposite films. The films were produced through a solvent casting method. The best results were achieved incorporating 0.8 wt % of carbon nanofiller, increasing the tensile strength by approximately 40% compared to biocomposites without GnPs. Additionally, the water vapor transmission rate decreased with the addition of a carbon-based nanofiller, while the thermal stability of the nanocomposite increased. Studies on unblended chitosan and starch were also performed by the same authors [186].

Mahmoudian and collaborators [182] prepared regenerated cellulose-GnPs nanocomposites using a solution casting method. At 3 wt % GnP concentration, the elastic modulus improved by 34%, and the tensile strength by 56%. The films also exhibited enhanced carbon dioxide and oxygen gas barrier properties. Gopiraman and collaborators [187] reinforced with GnPs cellulose acetate nanofibers produced by electrospinning. The diameter of the fiber decreased with increased filler amount. At 4 wt % concentrations, the biocomposite showed the highest Young's modulus (approximately 700 MPa), which was about 3.5 times higher than the pristine cellulose acetate fibrous mats. Thayumanavan et al. [183] mixed polyvinyl alcohol, sodium alginate, and GnPs by means of solvent-based techniques. They reported that sodium alginate helps the dispersion of GnPs inside the polymer matrix. By adding 0.5 wt % of nanofiller, they improved the tensile strength and modulus of pure polyvinyl alcohol by approximately 40% and 60% respectively. They obtained similar results by adding a surfactant during the preparation of GnP dispersions [188].

5.3. Reinforced Bioplastics Outlook

In summary, the field of GnPs-reinforced biopolymers is attracting attention. The reinforcement of commercially available bio-polyesters (i.e., PLA) is extensively investigated in light of the possible substitution of oil-derived plastics with bio-based ones. Indeed, today, numerous PLA-GnPs 3D-printable filaments [189] have already been produced by different companies, and are already

available in the market. Studies related to the reinforcement of other bio-polyesters such as PCL are still scarce. Indeed, the inclusion of GnPs inside PCL was mainly targeted for cell proliferation and tissue engineering [190,191]. Together with PCL, other biopolymers or natural polymers also reinforced with GnPs, such as starches and cellulosic materials, have good potential for the most demanding mechanical applications, but must be constantly improved. So far, GO was often coupled with such biopolymers, considering its superior chemical bonding with the host matrix; however, since GnPs theoretically have a higher Young's modulus [151], innovative techniques to incorporate GnPs in such biopolymers can pave the way for an enlargement of bioplastic-based structural applications.

6. Conclusions and Outlook

Graphene is foreseen as the breakthrough material of the 21st century. Nevertheless, since there is not a convenient mass-production method so far, other graphene-family products already industrially available are expanding in the market. In particular GnPs are receiving increased interest considering their nano-powder form and appealing chemo-physical properties, which make them a material of choice for advanced nanocomposites. In this review, we mostly concentrated on GnP-based emerging fields, such as flexible and wearable electronics, smart sensing, and reinforced biocomposites.

GnPs-based flexible electronics was thoroughly investigated and appears to have made a significant impact already. Many different approaches were proposed; freestanding GnP films and GnP inclusion in polymers are two examples. However, the most promising results were obtained so far by functionalizing flexible plastic substrates with pure nanoflakes or with polymer-GnPs conductive inks. With such approaches, researchers obtained durable and high-performance devices such as antennas, compliant electrodes for energy applications, and lightweight electromagnetic interference shielding films. Furthermore, extensive use of cellulose substrates, sometimes coupled with biopolymers, has been shown to be promising for the construction of sustainable flexible GnP-based technologies, and for an eco-friendly electronic waste management [192].

Wearable electronics require flexibility, foldability, stretchability, and washability, and at the same time, the ability to maintain a satisfactory electrical conductivity [48]. Nanocomposites, in general, are suitable for conductive wearable technologies [80] due to their intrinsic plastic mechanical properties and ease of manufacturing, and to the large spectra of properties accessible with different nanoparticles. Nonetheless, there is still the need for significant efforts to bring about the commercialization of reliable and washable GnP-based materials for innovative wearable and electrical conductive technologies. New and innovative approaches which bind conductive nanoflakes to textiles, even under severe mechanical stresses and laundry cycles, still need to be implemented.

In contrast, GnP-based smart sensing has already made promising progress. Ad-hoc material combinations that ensure stretchability and tunable electrical features appear to have made a significant impact as new generation wearable sensor technologies. In particular, since graphene-based material has exhibited one of the highest gauge factors ever reported, strain sensing mechanisms have somewhat matured for many uses, ranging from structural and human health monitoring to automotive and sports applications. So far, the combination of PDMS and GnPs were mainly explored, but there are further possibilities considering other elastomeric materials like thermoplastic polyurethanes, rubbers (e.g., nitrile and natural types), and gel-like constructs such as silly putty. Applications such as tactile devices and electronic robotic skins will benefit from the spread-out of GnPs-based smart sensors.

Last but not least, we reviewed the recent advances in GnP-reinforced biopolymer composites. There are already commercial products like skis or tires which benefits from GnP inclusion in oil-derived polymers. Lately, however, the need to reinforce biopolymers also emerged as a strategy to fill the performance gap between traditional long-lasting polymers and bioplastics. Through these strategies, wider use and larger scale use of biopolymers are targeted also for structural applications. PLA is the most investigated bioplastic coupled with GnPs. It has already shown satisfactory results. Indeed, there are already companies marketing GnPs-reinforced PLA 3D printing filaments. In contrast, additional efforts are required for effective GnP inclusion inside other bio-polyesters (like

polycaprolactone), starches, and cellulose-based materials. Considering all the results reviewed herein, and potential future developments, we believe that innovative materials and products based on GnPs in polymers will continue evolving towards commercialization and industrialization.

Funding: This research received no external funding.

Conflicts of Interest: The authors declare no conflicts of interest.

References

1. Novoselov, K.S.; Geim, A.K.; Morozov, S.; Jiang, D.; Katsnelson, M.; Grigorieva, I.; Dubonos, S.; Firsov, A.A. Two-dimensional gas of massless dirac fermions in grapheme. *Nature* **2005**, *438*, 197–200. [CrossRef] [PubMed]
2. Geim, A.K. Graphene: Status and prospects. *Science* **2009**, *324*, 1530–1534. [CrossRef] [PubMed]
3. Novoselov, K.S.; Geim, A.K.; Morozov, S.V.; Jiang, D.; Zhang, Y.; Dubonos, S.V.; Grigorieva, I.V.; Firsov, A.A. Electric field effect in atomically thin carbon films. *Science* **2004**, *306*, 666–669. [CrossRef] [PubMed]
4. Stankovich, S.; Dikin, D.A.; Piner, R.D.; Kohlhaas, K.A.; Kleinhammes, A.; Jia, Y.; Wu, Y.; Nguyen, S.T.; Ruoff, R.S. Synthesis of graphene-based nanosheets via chemical reduction of exfoliated graphite oxide. *Carbon* **2007**, *45*, 1558–1565. [CrossRef]
5. Ferrari, A.C.; Bonaccorso, F.; Fal'Ko, V.; Novoselov, K.S.; Roche, S.; Bøggild, P.; Borini, S.; Koppens, F.H.; Palermo, V.; Pugno, N.; et al. Science and technology roadmap for graphene, related two-dimensional crystals, and hybrid systems. *Nanoscale* **2015**, *7*, 4598–4810. [CrossRef] [PubMed]
6. Geim, A.K.; Novoselov, K.S. The rise of grapheme. *Nat. Mater.* **2007**, *6*, 183–191. [CrossRef] [PubMed]
7. Siochi, E.J. Graphene in the sky and beyond. *Nat. Nanotechnol.* **2014**, *9*, 745–747. [CrossRef] [PubMed]
8. Su, C.-Y.; Lu, A.-Y.; Xu, Y.; Chen, F.-R.; Khlobystov, A.N.; Li, L.-J. High-quality thin graphene films from fast electrochemical exfoliation. *ACS Nano* **2011**, *5*, 2332–2339. [CrossRef] [PubMed]
9. Bae, S.; Kim, H.; Lee, Y.; Xu, X.; Park, J.-S.; Zheng, Y.; Balakrishnan, J.; Lei, T.; Kim, H.R.; Song, Y.I.; et al. Roll-to-roll production of 30-inch graphene films for transparent electrodes. *Nat. Nanotechnol.* **2010**, *5*, 574–578. [CrossRef] [PubMed]
10. Novoselov, K.S.; Fal, V.; Colombo, L.; Gellert, P.; Schwab, M.; Kim, K. A roadmap for grapheme. *Nature* **2012**, *490*, 192–200. [CrossRef] [PubMed]
11. Park, S.; Ruoff, R.S. Chemical methods for the production of graphenes. *Nat. Nanotechnol.* **2009**, *4*, 217–224. [CrossRef] [PubMed]
12. Paton, K.R.; Varrla, E.; Backes, C.; Smith, R.J.; Khan, U.; O'Neill, A.; Boland, C.; Lotya, M.; Istrate, O.M.; King, P.; et al. Scalable production of large quantities of defect-free few-layer graphene by shear exfoliation in liquids. *Nat. Mater.* **2014**, *13*, 624–630. [CrossRef] [PubMed]
13. Chen, C.-H.; Yang, S.-W.; Chuang, M.-C.; Woon, W.-Y.; Su, C.-Y. Towards the continuous production of high crystallinity graphene via electrochemical exfoliation with molecular in situ encapsulation. *Nanoscale* **2015**, *7*, 15362–15373. [CrossRef] [PubMed]
14. Li, X.; Cai, W.; An, J.; Kim, S.; Nah, J.; Yang, D.; Piner, R.; Velamakanni, A.; Jung, I.; Tutuc, E.; et al. Large-area synthesis of high-quality and uniform graphene films on copper foils. *Science* **2009**, *324*, 1312–1314. [CrossRef] [PubMed]
15. Hernandez, Y.; Nicolosi, V.; Lotya, M.; Blighe, F.M.; Sun, Z.; De, S.; McGovern, I.; Holland, B.; Byrne, M.; Gun'Ko, Y.K.; et al. High-yield production of graphene by liquid-phase exfoliation of graphite. *Nat. Nanotechnol.* **2008**, *3*, 563–568. [CrossRef] [PubMed]
16. Lotya, M.; Hernandez, Y.; King, P.J.; Smith, R.J.; Nicolosi, V.; Karlsson, L.S.; Blighe, F.M.; De, S.; Wang, Z.; McGovern, I.; et al. Liquid phase production of graphene by exfoliation of graphite in surfactant/water solutions. *J. Am. Chem. Soc.* **2009**, *131*, 3611–3620. [CrossRef] [PubMed]
17. Young, R.J.; Kinloch, I.A.; Gong, L.; Novoselov, K.S. The mechanics of graphene nanocomposites: A review. *Compos. Sci. Technol.* **2012**, *72*, 1459–1476. [CrossRef]
18. Castillo, A.E.D.R.; Pellegrini, V.; Ansaldo, A.; Ricciardella, F.; Sun, H.; Marasco, L.; Buha, J.; Dang, Z.; Gagliani, L.; Lago, E.; et al. High-yield production of 2d crystals by wet-jet milling. *Mater. Horiz.* **2018**. [CrossRef]

19. Wick, P.; Louw-Gaume, A.E.; Kucki, M.; Krug, H.F.; Kostarelos, K.; Fadeel, B.; Dawson, K.A.; Salvati, A.; Vázquez, E.; Ballerini, L.; et al. Classification framework for graphene-based materials. *Angew. Chem. Int. Ed.* **2014**, *53*, 7714–7718. [CrossRef] [PubMed]
20. Jang, B.Z.; Zhamu, A. Processing of nanographene platelets (ngps) and ngp nanocomposites: A review. *J. Mater. Sci.* **2008**, *43*, 5092–5101. [CrossRef]
21. Sengupta, R.; Bhattacharya, M.; Bandyopadhyay, S.; Bhowmick, A.K. A review on the mechanical and electrical properties of graphite and modified graphite reinforced polymer composites. *Prog. Polym. Sci.* **2011**, *36*, 638–670. [CrossRef]
22. Yang, S.-Y.; Lin, W.-N.; Huang, Y.-L.; Tien, H.-W.; Wang, J.-Y.; Ma, C.-C.M.; Li, S.-M.; Wang, Y.-S. Synergetic effects of graphene platelets and carbon nanotubes on the mechanical and thermal properties of epoxy composites. *Carbon* **2011**, *49*, 793–803. [CrossRef]
23. Chung, D. A review of exfoliated graphite. *J. Mater. Sci.* **2016**, *51*, 554–568. [CrossRef]
24. Zhang, M.; Li, Y.; Su, Z.; Wei, G. Recent advances in the synthesis and applications of graphene–polymer nanocomposites. *Polym. Chem.* **2015**, *6*, 6107–6124. [CrossRef]
25. Shen, J.; Hu, Y.; Li, C.; Qin, C.; Ye, M. Synthesis of amphiphilic graphene nanoplatelets. *Small* **2009**, *5*, 82–85. [CrossRef] [PubMed]
26. Masood, M.T.; Papadopoulou, E.L.; Heredia-Guerrero, J.A.; Bayer, I.S.; Athanassiou, A.; Ceseracciu, L. Graphene and polytetrafluoroethylene synergistically improve the tribological properties and adhesion of nylon 66 coatings. *Carbon* **2017**, *123*, 26–33. [CrossRef]
27. Tabandeh-Khorshid, M.; Omrani, E.; Menezes, P.L.; Rohatgi, P.K. Tribological performance of self-lubricating aluminum matrix nanocomposites: Role of graphene nanoplatelets. *Eng. Sci. Technol. Int. J.* **2016**, *19*, 463–469. [CrossRef]
28. Das, A.; Kasaliwal, G.R.; Jurk, R.; Boldt, R.; Fischer, D.; Stöckelhuber, K.W.; Heinrich, G. Rubber composites based on graphene nanoplatelets, expanded graphite, carbon nanotubes and their combination: A comparative study. *Compos. Sci. Technol.* **2012**, *72*, 1961–1967. [CrossRef]
29. Prolongo, S.; Jimenez-Suarez, A.; Moriche, R.; Ureña, A. In situ processing of epoxy composites reinforced with graphene nanoplatelets. *Compos. Sci. Technol.* **2013**, *86*, 185–191. [CrossRef]
30. Rashad, M.; Pan, F.; Tang, A.; Asif, M. Effect of graphene nanoplatelets addition on mechanical properties of pure aluminum using a semi-powder method. *Prog. Natl. Sci. Mater. Int.* **2014**, *24*, 101–108. [CrossRef]
31. Yue, L.; Pircheraghi, G.; Monemian, S.A.; Manas-Zloczower, I. Epoxy composites with carbon nanotubes and graphene nanoplatelets–dispersion and synergy effects. *Carbon* **2014**, *78*, 268–278. [CrossRef]
32. Abbasi, A.; Sadeghi, G.M.M.; Ghasemi, I.; Shahrousvand, M. Shape memory performance of green in situ polymerized nanocomposites based on polyurethane/graphene nanoplatelets: Synthesis, properties, and cell behavior. *Polym. Compos.* **2017**. [CrossRef]
33. Lashgari, S.; Karrabi, M.; Ghasemi, I.; Azizi, H.; Messori, M.; Paderni, K. Shape memory nanocomposite of poly (L-lactic acid)/graphene nanoplatelets triggered by infrared light and thermal heating. *Express Polym. Lett.* **2016**, *10*, 349–359. [CrossRef]
34. Zhang, Z.-X.; Dou, J.-X.; He, J.-H.; Xiao, C.-X.; Shen, L.-Y.; Yang, J.-H.; Wang, Y.; Zhou, Z.-W. Electrically/infrared actuated shape memory composites based on a bio-based polyester blend and graphene nanoplatelets and their excellent self-driven ability. *J. Mater. Chem. C* **2017**, *5*, 4145–4158. [CrossRef]
35. Cui, Y.; Kundalwal, S.; Kumar, S. Gas barrier performance of graphene/polymer nanocomposites. *Carbon* **2016**, *98*, 313–333. [CrossRef]
36. Wu, H.; Drzal, L.T. Graphene nanoplatelet paper as a light-weight composite with excellent electrical and thermal conductivity and good gas barrier properties. *Carbon* **2012**, *50*, 1135–1145. [CrossRef]
37. Dittrich, B.; Wartig, K.-A.; Hofmann, D.; Mülhaupt, R.; Schartel, B. Flame retardancy through carbon nanomaterials: Carbon black, multiwall nanotubes, expanded graphite, multi-layer graphene and graphene in polypropylene. *Polym. Degrad. Stab.* **2013**, *98*, 1495–1505. [CrossRef]
38. Inuwa, I.; Hassan, A.; Wang, D.-Y.; Samsudin, S.; Haafiz, M.M.; Wong, S.; Jawaid, M. Influence of exfoliated graphite nanoplatelets on the flammability and thermal properties of polyethylene terephthalate/polypropylene nanocomposites. *Polym. Degrad. Stab.* **2014**, *110*, 137–148. [CrossRef]

39. Lin, C.; Chung, D. Graphite nanoplatelet pastes vs. carbon black pastes as thermal interface materials. *Carbon* **2009**, *47*, 295–305. [CrossRef]
40. Prolongo, S.; Moriche, R.; Jiménez-Suárez, A.; Sánchez, M.; Ureña, A. Epoxy adhesives modified with graphene for thermal interface materials. *J. Adhes.* **2014**, *90*, 835–847. [CrossRef]
41. Shtein, M.; Nadiv, R.; Buzaglo, M.; Kahil, K.; Regev, O. Thermally conductive graphene-polymer composites: Size, percolation, and synergy effects. *Chem. Mater.* **2015**, *27*, 2100–2106. [CrossRef]
42. Yadav, S.K.; Cho, J.W. Functionalized graphene nanoplatelets for enhanced mechanical and thermal properties of polyurethane nanocomposites. *Appl. Surf. Sci.* **2013**, *266*, 360–367. [CrossRef]
43. Cataldi, P.; Bayer, I.S.; Bonaccorso, F.; Pellegrini, V.; Athanassiou, A.; Cingolani, R. Foldable conductive cellulose fiber networks modified by graphene nanoplatelet-bio-based composites. *Adv. Electron. Mater.* **2015**, *1*. [CrossRef]
44. Jiang, X.; Drzal, L.T. Reduction in percolation threshold of injection molded high-density polyethylene/exfoliated graphene nanoplatelets composites by solid state ball milling and solid state shear pulverization. *J. Appl. Polym. Sci.* **2012**, *124*, 525–535. [CrossRef]
45. Sabzi, M.; Jiang, L.; Liu, F.; Ghasemi, I.; Atai, M. Graphene nanoplatelets as poly (lactic acid) modifier: Linear rheological behavior and electrical conductivity. *J. Mater. Chem. A* **2013**, *1*, 8253–8261. [CrossRef]
46. Yu, A.; Ramesh, P.; Sun, X.; Bekyarova, E.; Itkis, M.E.; Haddon, R.C. Enhanced thermal conductivity in a hybrid graphite nanoplatelet–carbon nanotube filler for epoxy composites. *Adv. Mater.* **2008**, *20*, 4740–4744. [CrossRef]
47. Shahil, K.M.; Balandin, A.A. Graphene–multilayer graphene nanocomposites as highly efficient thermal interface materials. *Nano Lett.* **2012**, *12*, 861–867. [CrossRef] [PubMed]
48. Jang, H.; Park, Y.J.; Chen, X.; Das, T.; Kim, M.-S.; Ahn, J.-H. Graphene-based flexible and stretchable electronics. *Adv. Mater.* **2016**, *28*, 4184–4202. [CrossRef] [PubMed]
49. Cummins, G.; Desmulliez, M.P. Inkjet printing of conductive materials: A review. *Circuit World* **2012**, *38*, 193–213. [CrossRef]
50. Yang, W.; Wang, C. Graphene and the related conductive inks for flexible electronics. *J. Mater. Chem. C* **2016**, *4*, 7193–7207. [CrossRef]
51. King, J.A.; Via, M.D.; Morrison, F.A.; Wiese, K.R.; Beach, E.A.; Cieslinski, M.J.; Bogucki, G.R. Characterization of exfoliated graphite nanoplatelets/polycarbonate composites: Electrical and thermal conductivity, and tensile, flexural, and rheological properties. *J. Compos. Mater.* **2012**, *46*, 1029–1039. [CrossRef]
52. Papadopoulou, E.L.; Pignatelli, F.; Marras, S.; Marini, L.; Davis, A.; Athanassiou, A.; Bayer, I.S. Nylon 6, 6/graphene nanoplatelet composite films obtained from a new solvent. *RSC Adv.* **2016**, *6*, 6823–6831. [CrossRef]
53. Hameed, N.; Dumée, L.F.; Allioux, F.-M.; Reghat, M.; Church, J.S.; Naebe, M.; Magniez, K.; Parameswaranpillai, J.; Fox, B.L. Graphene based room temperature flexible nanocomposites from permanently cross-linked networks. *Sci. Rep.* **2018**, *8*, 2803. [CrossRef] [PubMed]
54. Tian, M.; Huang, Y.; Wang, W.; Li, R.; Liu, P.; Liu, C.; Zhang, Y. Temperature-dependent electrical properties of graphene nanoplatelets film dropped on flexible substrates. *J. Mater. Res.* **2014**, *29*, 1288–1294. [CrossRef]
55. Wróblewski, G.; Janczak, D. Screen printed, transparent, and flexible electrodes based on graphene nanoplatelet pastes. In *Photonics Applications in Astronomy, Communications, Industry, and High-Energy Physics Experiments 2012*; International Society for Optics and Photonics: Bellingham, WA, USA, 2012; Volume 8454, p. 84541E.
56. Seekaew, Y.; Lokavee, S.; Phokharatkul, D.; Wisitsoraat, A.; Kerdcharoen, T.; Wongchoosuk, C. Low-cost and flexible printed graphene–pedot: Pss gas sensor for ammonia detection. *Org. Electron.* **2014**, *15*, 2971–2981. [CrossRef]
57. Huang, X.; Leng, T.; Chang, K.H.; Chen, J.C.; Novoselov, K.S.; Hu, Z. Graphene radio frequency and microwave passive components for low cost wearable electronics. *2D Mater.* **2016**, *3*, 025021. [CrossRef]
58. Mates, J.E.; Bayer, I.S.; Salerno, M.; Carroll, P.J.; Jiang, Z.; Liu, L.; Megaridis, C.M. Durable and flexible graphene composites based on artists' paint for conductive paper applications. *Carbon* **2015**, *87*, 163–174. [CrossRef]

59. Hyun, W.J.; Park, O.O.; Chin, B.D. Foldable graphene electronic circuits based on paper substrates. *Adv. Mater.* **2013**, *25*, 4729–4734. [CrossRef] [PubMed]
60. Scidà, A.; Haque, S.; Treossi, E.; Robinson, A.; Smerzi, S.; Ravesi, S.; Borini, S.; Palermo, V. Application of graphene-based flexible antennas in consumer electronic devices. *Mater. Today* **2018**, *21*, 223–230. [CrossRef]
61. Oh, J.S.; Oh, J.S.; Sung, D.I.; Yeom, G.Y. Fabrication of high-performance graphene nanoplatelet-based transparent electrodes via self-interlayer-exfoliation control. *Nanoscale* **2018**, *10*, 2351–2362. [CrossRef] [PubMed]
62. La Notte, L.; Cataldi, P.; Ceseracciu, L.; Bayer, I.S.; Athanassiou, A.; Marras, S.; Villari, E.; Brunetti, F.; Reale, A. Fully-sprayed flexible polymer solar cells with a cellulose-graphene electrode. *Mater. Today Energy* **2018**, *7*, 105–112. [CrossRef]
63. Cataldi, P.; Bonaccorso, F.; Castillo, A.E.D.; Pellegrini, V.; Jiang, Z.; Liu, L.; Boccardo, N.; Canepa, M.; Cingolani, R.; Athanassiou, A.; et al. Cellulosic graphene biocomposites for versatile high-performance flexible electronic applications. *Adv. Electron. Mater.* **2016**. [CrossRef]
64. Liu, X.; Zou, Q.; Wang, T.; Zhang, L. Electrically conductive graphene-based biodegradable polymer composite films with high thermal stability and flexibility. *Nano* **2018**, *13*, 1850033. [CrossRef]
65. Cataldi, P.; Bayer, I.S.; Nanni, G.; Athanassiou, A.; Bonaccorso, F.; Pellegrini, V.; Castillo, A.E.D.; Ricciardella, F.; Artyukhin, S.; Tronche, M.-A.; et al. Effect of graphene nano-platelet morphology on the elastic modulus of soft and hard biopolymers. *Carbon* **2016**, *109*, 331–339. [CrossRef]
66. Michel, M.; Biswas, C.; Tiwary, C.S.; Saenz, G.A.; Hossain, R.F.; Ajayan, P.; Kaul, A.B. A thermally-invariant, additively manufactured, high-power graphene resistor for flexible electronics. *2D Mater.* **2017**, *4*, 025076. [CrossRef]
67. Zhan, Y.; Lavorgna, M.; Buonocore, G.; Xia, H. Enhancing electrical conductivity of rubber composites by constructing interconnected network of self-assembled graphene with latex mixing. *J. Mater. Chem.* **2012**, *22*, 10464–10468. [CrossRef]
68. Irimia-Vladu, M. "Green" electronics: Biodegradable and biocompatible materials and devices for sustainable future. *Chem. Soc. Rev.* **2014**, *43*, 588–610. [CrossRef] [PubMed]
69. Irimia-Vladu, M.; Gowacki, E.D.; Voss, G.; Bauer, S.; Sariciftci, N.S. Green and biodegradable electronics. *Mater. Today* **2012**, *15*, 340–346. [CrossRef]
70. Stoppa, M.; Chiolerio, A. Wearable electronics and smart textiles: A critical review. *Sensors* **2014**, *14*, 11957–11992. [CrossRef] [PubMed]
71. Bao, Z.; Chen, X. Flexible and stretchable devices. *Adv. Mater.* **2016**, *28*, 4177–4179. [CrossRef] [PubMed]
72. Zeng, W.; Shu, L.; Li, Q.; Chen, S.; Wang, F.; Tao, X.-M. Fiber-based wearable electronics: A review of materials, fabrication, devices, and applications. *Adv. Mater.* **2014**, *26*, 5310–5336. [CrossRef] [PubMed]
73. Babu, K.F.; Dhandapani, P.; Maruthamuthu, S.; Kulandainathan, M.A. One pot synthesis of polypyrrole silver nanocomposite on cotton fabrics for multifunctional property. *Carbohydr. Polym.* **2012**, *90*, 1557–1563. [CrossRef] [PubMed]
74. Ji, X.; Xu, Y.; Zhang, W.; Cui, L.; Liu, J. Review of functionalization, structure and properties of graphene/polymer composite fibers. *Compos. Part A Appl. Sci. Manuf.* **2016**, *87*, 29–45. [CrossRef]
75. Neves, A.I.; Rodrigues, D.P.; Sanctis, A.; Alonso, E.T.; Pereira, M.S.; Amaral, V.S.; Melo, L.V.; Russo, S.; Schrijver, I.; Alves, H.; et al. Towards conductive textiles: Coating polymeric fibres with graphene. *Sci. Rep.* **2017**, *7*, 4250. [CrossRef] [PubMed]
76. Shateri-Khalilabad, M.; Yazdanshenas, M.E. Fabricating electroconductive cotton textiles using graphene. *Carbohydr. Polym.* **2013**, *96*, 190–195. [CrossRef] [PubMed]
77. Zhong, J.; Zhang, Y.; Zhong, Q.; Hu, Q.; Hu, B.; Wang, Z.L.; Zhou, J. Fiber-based generator for wearable electronics and mobile medication. *ACS Nano* **2014**, *8*, 6273–6280. [CrossRef] [PubMed]
78. Liu, W.-W.; Yan, X.-B.; Lang, J.-W.; Peng, C.; Xue, Q.-J. Flexible and conductive nanocomposite electrode based on graphene sheets and cotton cloth for supercapacitor. *J. Mater. Chem.* **2012**, *22*, 17245–17253. [CrossRef]
79. Windmiller, J.R.; Wang, J. Wearable electrochemical sensors and biosensors: A review. *Electroanalysis* **2013**, *25*, 29–46. [CrossRef]
80. Wagner, S.; Bauer, S. Materials for stretchable electronics. *Mrs Bull.* **2012**, *37*, 207–213. [CrossRef]

81. Molina, J. Graphene-based fabrics and their applications: A review. *RSC Adv.* **2016**, *6*, 68261–68291. [CrossRef]
82. Ren, J.; Wang, C.; Zhang, X.; Carey, T.; Chen, K.; Yin, Y.; Torrisi, F. Environmentally-friendly conductive cotton fabric as flexible strain sensor based on hot press reduced graphene oxide. *Carbon* **2017**, *111*, 622–630. [CrossRef]
83. Shateri-Khalilabad, M.; Yazdanshenas, M.E. Preparation of superhydrophobic electroconductive graphene-coated cotton cellulose. *Cellulose* **2013**, *20*, 963–972. [CrossRef]
84. Dong, Z.; Jiang, C.; Cheng, H.; Zhao, Y.; Shi, G.; Jiang, L.; Qu, L. Facile fabrication of light, flexible and multifunctional graphene fibers. *Adv. Mater.* **2012**, *24*, 1856–1861. [CrossRef] [PubMed]
85. Xu, Z.; Gao, C. Graphene fiber: A new trend in carbon fibers. *Mater. Today* **2015**, *18*, 480–492. [CrossRef]
86. Xu, Z.; Sun, H.; Zhao, X.; Gao, C. Ultrastrong fibers assembled from giant graphene oxide sheets. *Adv. Mater.* **2013**, *25*, 188–193. [CrossRef] [PubMed]
87. Neves, A.; Bointon, T.H.; Melo, L.; Russo, S.; de Schrijver, I.; Craciun, M.F.; Alves, H. Transparent conductive graphene textile fibers. *Sci. Rep.* **2015**, *5*, 9866. [CrossRef] [PubMed]
88. Yu, G.; Hu, L.; Vosgueritchian, M.; Wang, H.; Xie, X.; McDonough, J.R.; Cui, X.; Cui, Y.; Bao, Z. Solution-processed graphene/mno2 nanostructured textiles for high-performance electrochemical capacitors. *Nano Lett.* **2011**, *11*, 2905–2911. [CrossRef] [PubMed]
89. Woltornist, S.J.; Alamer, F.A.; McDannald, A.; Jain, M.; Sotzing, G.A.; Adamson, D.H. Preparation of conductive graphene/graphite infused fabrics using an interface trapping method. *Carbon* **2015**, *81*, 38–42. [CrossRef]
90. Sloma, M.; Janczak, D.; Wroblewski, G.; Mlozniak, A.; Jakubowska, M. Electroluminescent structures printed on paper and textile elastic substrates. *Circuit World* **2014**, *40*, 13–16. [CrossRef]
91. Tian, M.; Hu, X.; Qu, L.; Zhu, S.; Sun, Y.; Han, G. Versatile and ductile cotton fabric achieved via layer-by-layer self-assembly by consecutive adsorption of graphene doped pedot: Pss and chitosan. *Carbon* **2016**, *96*, 1166–1174. [CrossRef]
92. Skrzetuska, E.; Puchalski, M.; Krucinska, I. Chemically driven printed textile sensors based on graphene and carbon nanotubes. *Sensors* **2014**, *14*, 16816–16828. [CrossRef] [PubMed]
93. Cataldi, P.; Ceseracciu, L.; Athanassiou, A.; Bayer, I.S. Healable cotton–graphene nanocomposite conductor for wearable electronics. *ACS Appl. Mater. Interfaces* **2017**. [CrossRef] [PubMed]
94. Gong, S.; Cheng, W. One-dimensional nanomaterials for soft electronics. *Adv. Electron. Mater.* **2017**, *3*. [CrossRef]
95. Lu, N.; Kim, D.-H. Flexible and stretchable electronics paving the way for soft robotics. *Soft Robot.* **2014**, *1*, 53–62. [CrossRef]
96. Rogers, J.A.; Someya, T.; Huang, Y. Materials and mechanics for stretchable electronics. *Science* **2010**, *327*, 1603–1607. [CrossRef] [PubMed]
97. Yao, H.-B.; Ge, J.; Wang, C.-F.; Wang, X.; Hu, W.; Zheng, Z.-J.; Ni, Y.; Yu, S.-H. A flexible and highly pressure-sensitive graphene–polyurethane sponge based on fractured microstructure design. *Adv. Mater.* **2013**, *25*, 6692–6698. [CrossRef] [PubMed]
98. Park, M.; Park, J.; Jeong, U. Design of conductive composite elastomers for stretchable electronics. *Nano Today* **2014**, *9*, 244–260. [CrossRef]
99. Yao, S.; Zhu, Y. Nanomaterial-enabled stretchable conductors: Strategies, materials and devices. *Adv. Mater.* **2015**, *27*, 1480–1511. [CrossRef] [PubMed]
100. Yuan, X.; Wei, Y.; Chen, S.; Wang, P.; Liu, L. Bio-based graphene/sodium alginate aerogels for strain sensors. *RSC Adv.* **2016**, *6*, 64056–64064. [CrossRef]
101. Boland, C.S.; Khan, U.; Backes, C.; O'Neill, A.; McCauley, J.; Duane, S.; Shanker, R.; Liu, Y.; Jurewicz, I.; Dalton, A.B.; et al. Sensitive, high-strain, high-rate bodily motion sensors based on graphene–rubber composites. *ACS Nano* **2014**, *8*, 8819–8830. [CrossRef] [PubMed]
102. Jason, N.N.; Wang, S.J.; Bhanushali, S.; Cheng, W. Skin inspired fractal strain sensors using a copper nanowire and graphite microflake hybrid conductive network. *Nanoscale* **2016**, *8*, 16596–16605. [CrossRef] [PubMed]
103. Li, X.; Zhang, R.; Yu, W.; Wang, K.; Wei, J.; Wu, D.; Cao, A.; Li, Z.; Cheng, Y.; Zheng, Q.; et al. Stretchable and highly sensitive graphene-on-polymer strain sensors. *Sci. Rep.* **2012**, *2*, 870. [CrossRef] [PubMed]

104. Hempel, M.; Nezich, D.; Kong, J.; Hofmann, M. A novel class of strain gauges based on layered percolative films of 2d materials. *Nano Lett.* **2012**, *12*, 5714–5718. [CrossRef] [PubMed]
105. Cataldi, P.; Dussoni, S.; Ceseracciu, L.; Maggiali, M.; Natale, L.; Metta, G.; Athanassiou, A.; Bayer, I.S. Carbon nanofiber versus graphene-based stretchable capacitive touch sensors for artificial electronic skin. *Adv. Sci.* **2018**, *5*. [CrossRef] [PubMed]
106. Zahid, M.; Papadopoulou, E.L.; Athanassiou, A.; Bayer, I.S. Strain-responsive mercerized conductive cotton fabrics based on pedot: Pss/graphene. *Mater. Des.* **2017**, *135*, 213–222. [CrossRef]
107. Moriche, R.; Sanchez, M.; Jiménez-Suárez, A.; Prolongo, S.; Urena, A. Strain monitoring mechanisms of sensors based on the addition of graphene nanoplatelets into an epoxy matrix. *Compos. Sci. Technol.* **2016**, *123*, 65–70. [CrossRef]
108. Moriche, R.; Sánchez, M.; Prolongo, S.G.; Jiménez-Suárez, A.; Ureña, A. Reversible phenomena and failure localization in self-monitoring gnp/epoxy nanocomposites. *Compos. Struct.* **2016**, *136*, 101–105. [CrossRef]
109. Wang, B.; Lee, B.-K.; Kwak, M.-J.; Lee, D.-W. Graphene/polydimethylsiloxane nanocomposite strain sensor. *Rev. Sci. Instrum.* **2013**, *84*, 105005. [CrossRef] [PubMed]
110. Boland, C.S.; Khan, U.; Ryan, G.; Barwich, S.; Charifou, R.; Harvey, A.; Backes, C.; Li, Z.; Ferreira, M.S.; Möbius, M.E.; et al. Sensitive electromechanical sensors using viscoelastic graphene-polymer nanocomposites. *Science* **2016**, *354*, 1257–1260. [CrossRef] [PubMed]
111. Cataldi, P.; Ceseracciu, L.; Marras, S.; Athanassiou, A.; Bayer, I.S. Electrical conductivity enhancement in thermoplastic polyurethane-graphene nanoplatelet composites by stretch-release cycles. *Appl. Phys. Lett.* **2017**, *110*, 121904. [CrossRef]
112. Lee, C.; Jug, L.; Meng, E. High strain biocompatible polydimethylsiloxane-based conductive graphene and multiwalled carbon nanotube nanocomposite strain sensors. *Appl. Phys. Lett.* **2013**, *102*, 183511. [CrossRef]
113. Janczak, D.; Soma, M.; Wróblewski, G.; Mozniak, A.; Jakubowska, M. Screen-printed resistive pressure sensors containing graphene nanoplatelets and carbon nanotubes. *Sensors* **2014**, *14*, 17304–17312. [CrossRef] [PubMed]
114. Moriche, R.; Jiménez-Suárez, A.; Sánchez, M.; Prolongo, S.; Ureña, A. Graphene nanoplatelets coated glass fibre fabrics as strain sensors. *Compos. Sci. Technol.* **2017**, *146*, 59–64. [CrossRef]
115. Moriche, R.; Jiménez-Suárez, A.; Sánchez, M.; Prolongo, S.; Ureña, A. Sensitivity, influence of the strain rate and reversibility of gnps based multiscale composite materials for high sensitive strain sensors. *Compos. Sci. Technol.* **2018**, *155*, 100–107. [CrossRef]
116. Park, J.J.; Hyun, W.J.; Mun, S.C.; Park, Y.T.; Park, O.O. Highly stretchable and wearable graphene strain sensors with controllable sensitivity for human motion monitoring. *ACS Appl. Mater. Interfaces* **2015**, *7*, 6317–6324. [CrossRef] [PubMed]
117. Shi, G.; Zhao, Z.; Pai, J.-H.; Lee, I.; Zhang, L.; Stevenson, C.; Ishara, K.; Zhang, R.; Zhu, H.; Ma, J. Highly sensitive, wearable, durable strain sensors and stretchable conductors using graphene/silicon rubber composites. *Adv. Funct. Mater.* **2016**, *26*, 7614–7625. [CrossRef]
118. Zhao, H.; Bai, J. Highly sensitive piezo-resistive graphite nanoplatelet–carbon nanotube hybrids/polydimethylsilicone composites with improved conductive network construction. *ACS Appl. Mater. Interfaces* **2015**, *7*, 9652–9659. [CrossRef] [PubMed]
119. Filippidou, M.; Tegou, E.; Tsouti, V.; Chatzandroulis, S. A flexible strain sensor made of graphene nanoplatelets/polydimethylsiloxane nanocomposite. *Microelectron. Eng.* **2015**, *142*, 7–11. [CrossRef]
120. Rinaldi, A.; Tamburrano, A.; Fortunato, M.; Sarto, M.S. A flexible and highly sensitive pressure sensor based on a pdms foam coated with graphene nanoplatelets. *Sensors* **2016**, *16*, 2148. [CrossRef] [PubMed]
121. Moriche, R.; Prolongo, S.G.; Sánchez, M.; Jiménez-Suárez, A.; Campo, M.; Ureña, A. Strain sensing based on multiscale composite materials reinforced with graphene nanoplatelets. *J. Vis. Exp. JoVE* **2016**. [CrossRef] [PubMed]
122. Yan, C.; Wang, J.; Kang, W.; Cui, M.; Wang, X.; Foo, C.Y.; Chee, K.J.; Lee, P.S. Highly stretchable piezoresistive graphene–nanocellulose nanopaper for strain sensors. *Adv. Mater.* **2014**, *26*, 2022–2027. [CrossRef] [PubMed]
123. Kim, Y.-J.; Cha, J.Y.; Ham, H.; Huh, H.; So, D.-S.; Kang, I. Preparation of piezoresistive nano smart hybrid material based on graphene. *Curr. Appl. Phys.* **2011**, *11*, S350–S352. [CrossRef]

124. Tadakaluru, S.; Thongsuwan, W.; Singjai, P. Stretchable and flexible high-strain sensors made using carbon nanotubes and graphite films on natural rubber. *Sensors* **2014**, *14*, 868–876. [CrossRef] [PubMed]
125. Amjadi, M.; Pichitpajongkit, A.; Lee, S.; Ryu, S.; Park, I. Highly stretchable and sensitive strain sensor based on silver nanowire–elastomer nanocomposite. *ACS Nano* **2014**, *8*, 5154–5163. [CrossRef] [PubMed]
126. Jeong, Y.R.; Park, H.; Jin, S.W.; Hong, S.Y.; Lee, S.-S.; Ha, J.S. Highly stretchable and sensitive strain sensors using fragmentized graphene foam. *Adv. Funct. Mater.* **2015**, *25*, 4228–4236. [CrossRef]
127. Lee, J.; Kim, S.; Lee, J.; Yang, D.; Park, B.C.; Ryu, S.; Park, I. A stretchable strain sensor based on a metal nanoparticle thin film for human motion detection. *Nanoscale* **2014**, *6*, 11932–11939. [CrossRef] [PubMed]
128. Lötters, J.C.; Olthuis, W.; Veltink, P.; Bergveld, P. The mechanical properties of the rubber elastic polymer polydimethylsiloxane for sensor applications. *J. Micromechan. Microeng.* **1997**, *7*, 145–147. [CrossRef]
129. Lu, N.; Lu, C.; Yang, S.; Rogers, J. Highly sensitive skin-mountable strain gauges based entirely on elastomers. *Adv. Funct. Mater.* **2012**, *22*, 4044–4050. [CrossRef]
130. Yamada, T.; Hayamizu, Y.; Yamamoto, Y.; Yomogida, Y.; Izadi-Najafabadi, A.; Futaba, D.N.; Hata, K. A stretchable carbon nanotube strain sensor for human-motion detection. *Nat. Nanotechnol.* **2011**, *6*, 296–301. [CrossRef] [PubMed]
131. Lee, S.W.; Park, J.J.; Park, B.H.; Mun, S.C.; Park, Y.T.; Liao, K.; Seo, T.S.; Hyun, W.J.; Park, O.O. Enhanced sensitivity of patterned graphene strain sensors used for monitoring subtle human body motions. *ACS Appl. Mater. Interfaces* **2017**, *9*, 11176–11183. [CrossRef] [PubMed]
132. Liu, H.; Li, Y.; Dai, K.; Zheng, G.; Liu, C.; Shen, C.; Yan, X.; Guo, J.; Guo, Z. Electrically conductive thermoplastic elastomer nanocomposites at ultralow graphene loading levels for strain sensor applications. *J. Mater. Chem. C* **2016**, *4*, 157–166. [CrossRef]
133. Cheng, Y.; Wang, R.; Sun, J.; Gao, L. A stretchable and highly sensitive graphene-based fiber for sensing tensile strain, bending, and torsion. *Adv. Mater.* **2015**, *27*, 7365–7371. [CrossRef] [PubMed]
134. Rams, J.; Sanchez, M.; Urena, A.; Jimenez-Suarez, A.; Campo, M.; Güemes, A. Use of carbon nanotubes for strain and damage sensing of epoxy-based composites. *Int. J. Smart Nano Mater.* **2012**, *3*, 152–161. [CrossRef]
135. Schmitz, A.; Maiolino, P.; Maggiali, M.; Natale, L.; Cannata, G.; Metta, G. Methods and technologies for the implementation of large-scale robot tactile sensors. *IEEE Trans. Robot.* **2011**, *27*, 389–400. [CrossRef]
136. Zhang, N.; Luan, P.; Zhou, W.; Zhang, Q.; Cai, L.; Zhang, X.; Zhou, W.; Fan, Q.; Yang, F.; Zhao, D.; et al. Highly stretchable pseudocapacitors based on buckled reticulate hybrid electrodes. *Nano Res.* **2014**, *7*, 1680–1690. [CrossRef]
137. Das, T.K.; Prusty, S. Graphene-based polymer composites and their applications. *Polym.-Plast. Technol. Eng.* **2013**, *52*, 319–331. [CrossRef]
138. Kim, H.; Abdala, A.A.; Macosko, C.W. Graphene/polymer nanocomposites. *Macromolecules* **2010**, *43*, 6515–6530. [CrossRef]
139. Kuilla, T.; Bhadra, S.; Yao, D.; Kim, N.H.; Bose, S.; Lee, J.H. Recent advances in graphene based polymer composites. *Prog. Polym. Sci.* **2010**, *35*, 1350–1375. [CrossRef]
140. Mukhopadhyay, P.; Gupta, R.K. Trends and frontiers in graphene-based polymer nanocomposites. *Plast. Eng.* **2011**, *67*, 32–42.
141. Rafiee, M.A. Graphene-Based Composite Materials. Ph.D. Thesis, Rensselaer Polytechnic Institute, Troy, NY, USA, 2011.
142. Hu, K.; Kulkarni, D.D.; Choi, I.; Tsukruk, V.V. Graphene-polymer nanocomposites for structural and functional applications. *Prog. Polym. Sci.* **2014**, *39*, 1934–1972. [CrossRef]
143. Karevan, M.; Kalaitzidou, K. Understanding the property enhancement mechanism in exfoliated graphite nanoplatelets reinforced polymer nanocomposites. *Compos. Interfaces* **2013**, *20*, 255–268. [CrossRef]
144. Zaman, I.; Manshoor, B.; Khalid, A.; Araby, S. From clay to graphene for polymer nanocomposites: A survey. *J. Polym. Res.* **2014**, *21*, 429. [CrossRef]
145. Dimov, D.; Amit, I.; Gorrie, O.; Barnes, M.D.; Townsend, N.J.; Neves, A.I.; Withers, F.; Russo, S.; Craciun, M.F. Ultrahigh performance nanoengineered graphene–concrete composites for multifunctional applications. *Adv. Funct. Mater.* **2018**, 1705183. [CrossRef]
146. Böhm, S. Graphene against corrosion. *Nat. Nanotechnol.* **2014**, *9*, 741–742. [CrossRef] [PubMed]

147. Elmarakbi, A.; Azoti, W. Novel composite materials for automotive applications: Concepts and challenges for energy-efficient and safe vehicles. In Proceedings of the 10th International Conference on Composite Science and Technology, Lisbon, Portugal, 2–4 September 2015.
148. Rafiee, M.; Rafiee, J.; Yu, Z.-Z.; Koratkar, N. Buckling resistant graphene nanocomposites. *Appl. Phys. Lett.* **2009**, *95*, 223103. [CrossRef]
149. Das, D.; Swain, P.; Sahoo, S. Graphene in turbine blades. *Modern Phys. Lett. B* **2016**, *30*, 1650262. [CrossRef]
150. Yavari, F.; Rafiee, M.; Rafiee, J.; Yu, Z.-Z.; Koratkar, N. Dramatic increase in fatigue life in hierarchical graphene composites. *ACS Appl. Mater. Interfaces* **2010**, *2*, 2738–2743. [CrossRef] [PubMed]
151. Ma, J.; Meng, Q.; Zaman, I.; Zhu, S.; Michelmore, A.; Kawashima, N.; Wang, C.H.; Kuan, H.-C. Development of polymer composites using modified, high-structural integrity graphene platelets. *Compos. Sci. Technol.* **2014**, *91*, 82–90. [CrossRef]
152. Rafiee, M.A.; Rafiee, J.; Wang, Z.; Song, H.; Yu, Z.-Z.; Koratkar, N. Enhanced mechanical properties of nanocomposites at low graphene content. *ACS Nano* **2009**, *3*, 3884–3890. [CrossRef] [PubMed]
153. Mittal, G.; Dhand, V.; Rhee, K.Y.; Park, S.-J.; Lee, W.R. A review on carbon nanotubes and graphene as fillers in reinforced polymer nanocomposites. *J. Ind. Eng. Chem.* **2015**, *21*, 11–25. [CrossRef]
154. Boothroyd, S.C.; Johnson, D.W.; Weir, M.P.; Reynolds, C.D.; Hart, J.M.; Smith, A.J.; Clarke, N.; Thompson, R.L.; Coleman, K.S. Controlled structure evolution of graphene networks in polymer composites. *Chem. Mater.* **2018**, *30*, 1524–1530. [CrossRef]
155. Sun, X.; Sun, H.; Li, H.; Peng, H. Developing polymer composite materials: Carbon nanotubes or graphene? *Adv. Mater.* **2013**, *25*, 5153–5176. [CrossRef] [PubMed]
156. Tang, L.-C.; Wan, Y.-J.; Yan, D.; Pei, Y.-B.; Zhao, L.; Li, Y.-B.; Wu, L.-B.; Jiang, J.-X.; Lai, G.-Q. The effect of graphene dispersion on the mechanical properties of graphene/epoxy composites. *Carbon* **2013**, *60*, 16–27. [CrossRef]
157. Moriche, R.; Prolongo, S.; Sánchez, M.; Jiménez-Suárez, A.; Sayagués, M.; Ureña, A. Morphological changes on graphene nanoplatelets induced during dispersion into an epoxy resin by different methods. *Compos. Part B Eng.* **2015**, *72*, 199–205. [CrossRef]
158. Prolongo, S.; Jiménez-Suárez, A.; Moriche, R.; Ureña, A. Graphene nanoplatelets thickness and lateral size influence on the morphology and behavior of epoxy composites. *Eur. Polym. J.* **2014**, *53*, 292–301. [CrossRef]
159. Papageorgiou, D.G.; Kinloch, I.A.; Young, R.J. Mechanical properties of graphene and graphene-based nanocomposites. *Prog. Mater. Sci.* **2017**, *90*, 75–127. [CrossRef]
160. Bayer, I.S. Thermomechanical properties of polylactic acid-graphene composites: A state-of-the-art review for biomedical applications. *Materials* **2017**, *10*, 748. [CrossRef] [PubMed]
161. Heredia-Guerrero, J.A.; Bentez, J.J.; Cataldi, P.; Paul, U.C.; Contardi, M.; Cingolani, R.; Bayer, I.S.; Heredia, A.; Athanassiou, A. All-natural sustainable packaging materials inspired by plant cuticles. *Adv. Sustain. Syst.* **2017**, 1. [CrossRef]
162. Scaffaro, R.; Botta, L.; Maio, A.; Mistretta, M.C.; la Mantia, F.P. Effect of graphene nanoplatelets on the physical and antimicrobial properties of biopolymer-based nanocomposites. *Materials* **2016**, *9*, 351. [CrossRef] [PubMed]
163. Bordes, P.; Pollet, E.; Avérous, L. Nano-biocomposites: Biodegradable polyester/nanoclay systems. *Prog. Polym. Sci.* **2009**, *34*, 125–155. [CrossRef]
164. Raquez, J.-M.; Habibi, Y.; Murariu, M.; Dubois, P. Polylactide (pla)-based nanocomposites. *Prog. Polym. Sci.* **2013**, *38*, 1504–1542. [CrossRef]
165. Sriprachuabwong, C.; Duangsripat, S.; Sajjaanantakul, K.; Wisitsoraat, A.; Tuantranont, A. Electrolytically exfoliated graphene–polylactide-based bioplastic with high elastic performance. *J. Appl. Polym. Sci.* **2015**, *132*. [CrossRef]
166. Botta, L.; Scaffaro, R.; Mistretta, M.; la Mantia, F. Biopolymer based nanocomposites reinforced with graphene nanoplatelets. *AIP Conf. Proc.* **2016**, *1736*, 020156.
167. Rouf, T.B.; Kokini, J.L. Biodegradable biopolymer–graphene nanocomposites. *J. Mater. Sci.* **2016**, *51*, 9915–9945. [CrossRef]
168. Mittal, V.; Chaudhry, A.U.; Luckachan, G.E. Biopolymer–thermally reduced graphene nanocomposites: Structural characterization and properties. *Mater. Chem. Phys.* **2014**, *147*, 319–332. [CrossRef]

169. Ionită, M.; Vlăsceanu, G.M.; Watzlawek, A.A.; Voicu, S.I.; Burns, J.S.; Iovu, H. Graphene and functionalized graphene: Extraordinary prospects for nanobiocomposite materials. *Compos. Part B Eng.* **2017**, *121*, 34–57. [CrossRef]
170. Gonçalves, C.; Pinto, A.; Machado, A.V.; Moreira, J.; Gonçalves, I.C.; Magalhães, F. Biocompatible reinforcement of poly (lactic acid) with graphene nanoplatelets. *Polym. Compos.* **2016**. [CrossRef]
171. Scaffaro, R.; Botta, L.; Maio, A.; Gallo, G. Pla graphene nanoplatelets nanocomposites: Physical properties and release kinetics of an antimicrobial agent. *Compos. Part B Eng.* **2017**, *109*, 138–146. [CrossRef]
172. Chieng, B.W.; Ibrahim, N.A.; Yunus, W.M.Z.W.; Hussein, M.Z.; Loo, Y.Y. Effect of graphene nanoplatelets as nanofiller in plasticized poly (lactic acid) nanocomposites. *J. Ther. Anal. Calorim.* **2014**, *118*, 1551–1559. [CrossRef]
173. Chieng, B.W.; Ibrahim, N.A.; Yunus, W.M.Z.W.; Hussein, M.Z. Poly (lactic acid)/poly (ethylene glycol) polymer nanocomposites: Effects of graphene nanoplatelets. *Polymers* **2013**, *6*, 93–104. [CrossRef]
174. Chieng, B.W.; Ibrahim, N.A.; Yunus, W.M.Z.W.; Hussein, M.Z.; Then, Y.Y.; Loo, Y.Y. Reinforcement of graphene nanoplatelets on plasticized poly (lactic acid) nanocomposites: Mechanical, thermal, morphology, and antibacterial properties. *J. Appl. Polym. Sci.* **2015**, *132*. [CrossRef]
175. Narimissa, E.; Gupta, R.K.; Choi, H.J.; Kao, N.; Jollands, M. Morphological, mechanical, and thermal characterization of biopolymer composites based on polylactide and nanographite platelets. *Polym. Compos.* **2012**, *33*, 1505–1515. [CrossRef]
176. Narimissa, E.; Gupta, R.K.; Kao, N.; Choi, H.J.; Jollands, M.; Bhattacharya, S.N. Melt rheological investigation of polylactide-nanographite platelets biopolymer composites. *Polym. Eng. Sci.* **2014**, *54*, 175–188. [CrossRef]
177. Gao, Y.; Picot, O.T.; Bilotti, E.; Peijs, T. Influence of filler size on the properties of poly (lactic acid)(pla)/graphene nanoplatelet (gnp) nanocomposites. *Eur. Polym. J.* **2017**, *86*, 117–131. [CrossRef]
178. Pinto, A.M.; Cabral, J.; Tanaka, D.A.P.; Mendes, A.M.; Magalhães, F.D. Effect of incorporation of graphene oxide and graphene nanoplatelets on mechanical and gas permeability properties of poly (lactic acid) films. *Polym. Int.* **2013**, *62*, 33–40. [CrossRef]
179. Chieng, B.W.; Ibrahim, N.A.; Yunus, W.M.Z.W.; Hussein, M.Z.; Then, Y.Y.; Loo, Y.Y. Effects of graphene nanoplatelets and reduced graphene oxide on poly (lactic acid) and plasticized poly (lactic acid): A comparative study. *Polymers* **2014**, *6*, 2232–2246. [CrossRef]
180. Wang, M.; Deng, X.-Y.; Du, A.-K.; Zhao, T.-H.; Zeng, J.-B. Poly (sodium 4-styrenesulfonate) modified graphene for reinforced biodegradable poly (-caprolactone) nanocomposites. *RSC Adv.* **2015**, *5*, 73146–73154. [CrossRef]
181. Ashori, A.; Bahrami, R. Modification of physico-mechanical properties of chitosan-tapioca starch blend films using nano graphene. *Polym. Plast. Technol. Eng.* **2014**, *53*, 312–318. [CrossRef]
182. Mahmoudian, S.; Wahit, M.U.; Imran, M.; Ismail, A.; Balakrishnan, H. A facile approach to prepare regenerated cellulose/graphene nanoplatelets nanocomposite using room-temperature ionic liquid. *J. Nanosci. Nanotechnol.* **2012**, *12*, 5233–5239. [CrossRef] [PubMed]
183. Thayumanavan, N.; Tambe, P.; Joshi, G.; Shukla, M. Effect of sodium alginate modification of graphene (by "anion-π" type of interaction) on the mechanical and thermal properties of polyvinyl alcohol (pva) nanocomposites. *Compos. Interfaces* **2014**, *21*, 487–506. [CrossRef]
184. Pinto, A.M.; Moreira, S.; Gonçalves, I.C.; Gama, F.M.; Mendes, A.M.; Magalhães, F.D. Biocompatibility of poly (lactic acid) with incorporated graphene-based materials. *Colloids Surf. B Biointerfaces* **2013**, *104*, 229–238. [CrossRef] [PubMed]
185. Pinto, A.M.; Goncalves, I.C.; Magalhães, F.D. Graphene-based materials biocompatibility: A review. *Colloids Surf. B Biointerfaces* **2013**, *111*, 188–202. [CrossRef] [PubMed]
186. Ashori, A. Effects of graphene on the behavior of chitosan and starch nanocomposite films. *Polym. Eng. Sci.* **2014**, *54*, 2258–2263. [CrossRef]
187. Gopiraman, M.; Fujimori, K.; Zeeshan, K.; Kim, B.; Kim, I. Structural and mechanical properties of cellulose acetate/graphene hybrid nanofibers: Spectroscopic investigations. *Express Polym. Lett.* **2013**, *7*, 554–564. [CrossRef]
188. Thayumanavan, N.; Tambe, P.; Joshi, G. Effect of surfactant and sodium alginate modification of graphene on the mechanical and thermal properties of polyvinyl alcohol (pva) nanocomposites. *Cell. Chem. Technol.* **2015**, *49*, 69–80.

189. Bustillos, J.; Montero, D.; Nautiyal, P.; Loganathan, A.; Boesl, B.; Agarwal, A. Integration of graphene in poly (lactic) acid by 3d printing to develop creep and wear-resistant hierarchical nanocomposites. *Polym. Compos.* **2017**. [CrossRef]
190. Qian, Y.; Zhao, X.; Han, Q.; Chen, W.; Li, H.; Yuan, W. An integrated multi-layer 3d-fabrication of pda/rgd coated graphene loaded pcl nanoscaffold for peripheral nerve restoration. *Nat. Commun.* **2018**, *9*, 323. [CrossRef] [PubMed]
191. Wang, W.; Caetano, G.; Ambler, W.S.; Blaker, J.J.; Frade, M.A.; Mandal, P.; Diver, C.; Bártolo, P. Enhancing the hydrophilicity and cell attachment of 3d printed pcl/graphene scaffolds for bone tissue engineering. *Materials* **2016**, *9*, 992. [CrossRef] [PubMed]
192. Cataldi, P.; Heredia-Guerrero, J.A.; Guzman-Puyol, S.; Ceseracciu, L.; La Notte, L.; Reale, A.; Ren, J.; Zhang, Y.; Liu, L.; Miscuglio, M.; et al. Sustainable Electronics Based on Crop Plant Extracts and Graphene: A "Bioadvantaged" Approach. *Adv. Sustain. Syst.* **2018**, 1800069. [CrossRef]